

AD-A102 944

WYOMING UNIV LARAMIE DEPT OF ATMOSPHERIC SCIENCE  
CONDUCT OF CLOUD SPECTRA MEASUREMENTS.(U)  
FEB 81 G VALI, M K POLITOVICH

F/G 4/1

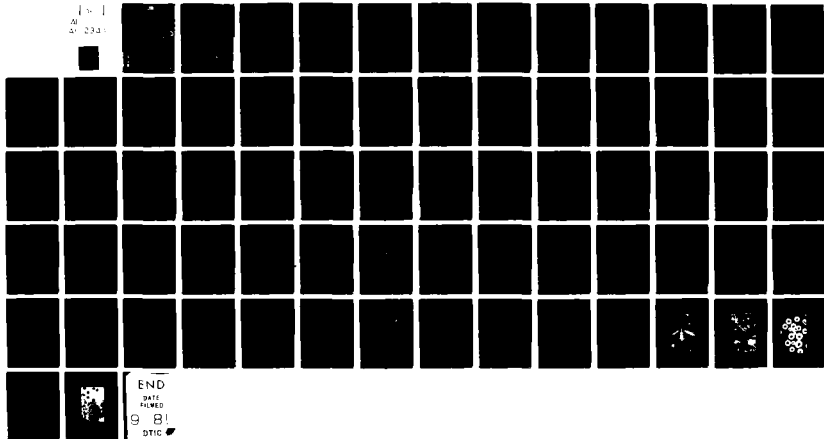
F19628-79-C-0029

UNCLASSIFIED

AFGL-TR-81-0122

NL

1-1  
AD 2341



A081127

LEVEL

AFGL-TR-81-0122

2

AD A102944

# CONDUCT OF CLOUD SPECTRA MEASUREMENTS

Gabor Vali  
Marcia K. Politovich  
Darrel G. Baumgardner

University of Wyoming  
Department of Atmospheric Science  
P.O. Box 3038  
Laramie, Wyoming 82071

Final Report  
1 October 1979 - 30 September 1980

DTIC  
AUG 17 1981  
H

6 February 1981

Approved for public release; distribution unlimited

AIR FORCE GEOPHYSICS LABORATORY  
AIR FORCE SYSTEMS COMMAND  
UNITED STATES AIR FORCE  
HANSOM AFB, MASSACHUSETTS 01731

FILE COPY

81 8 17 057

Qualified requestors may obtain additional copies from the  
Defense Technical Information Center. All others should  
apply to the National Technical Information Service.

UNCLASSIFIED

SECURITY CLASSIFICATION OF THIS PAGE (When Data Entered)

| REPORT DOCUMENTATION PAGE  |                                     | READ INSTRUCTIONS<br>BEFORE COMPLETING FORM   |
|--|-------------------------------------|---|
| 1. REPORT NUMBER<br>AFGL-TR-81-0122  | 2. GOVT ACCESSION NO.<br>AD-A102944 | 3. REPORT NUMBER CATALOG NUMBER   |
| 4. TITLE (and Subtitle)<br>CONDUCT OF CLOUD SPECTRA MEASUREMENTS   |                                     | 5. TYPE OF REPORT & PERIOD COVERED<br>Final Scientific Report<br>1 Oct 1979 - 30 Sep 1980 |
| 7. AUTHOR(s)<br>Gabor Vali<br>Marcia K. Politovich<br>Darrel G. Baumgardner  |                                     | 6. PERFORMING ORG. REPORT NUMBER  |
| 9. PERFORMING ORGANIZATION NAME AND ADDRESS  |                                     | 8. CONTRACT OR GRANT NUMBER(s)<br>F19628-79-C-0029  |
| 11. CONTROLLING OFFICE NAME AND ADDRESS<br>University of Wyoming<br>Dept of Atmospheric Science, P O Box 3038<br>Laramie, Wyoming 82071  |                                     | 10. PROGRAM ELEMENT, PROJECT, TASK<br>AREA & WORK UNIT NUMBERS<br>62101F<br>667012AA      |
| 14. MONITORING AGENCY NAME & ADDRESS (if different from Controlling Office)<br>Air Force Geophysics Laboratory<br>Hanscom AFB MA 10731<br>Monitor/Rosemary M. Dyer/LYC   |                                     | 12. REPORT DATE<br>6 Feb 1981   |
|  |                                     | 13. NUMBER OF PAGES<br>69   |
|  |                                     | 15. SECURITY CLASS. (of this report)<br>UNCLASSIFIED                                      |
| 16. DISTRIBUTION STATEMENT (of this Report)<br>Approved for Public Release Distribution Unlimited  |                                     | 15a. DECLASSIFICATION/DOWNGRADING<br>SCHEDULE   |
| 17. DISTRIBUTION STATEMENT (of the abstract entered in Block 20, if different from Report)   |                                     |   |
| 18. SUPPLEMENTARY NOTES  |                                     |   |
| 19. KEY WORDS (Continue on reverse side if necessary and identify by block number)<br>Cloud Physics Instrumentation<br>Cloud Particle Spectra<br>Liquid Water Content  |                                     |   |
| 20. ABSTRACT (Continue on reverse side if necessary and identify by block number)<br>The reasons for instrumental errors in cloud particle spectra and liquid water measurements were investigated. Calibrations and tests were performed on four probes manufactured by Particle Measuring Systems (PMS) and on a hot-wire liquid water device designed at CSIRO and built at the University of Wyoming.<br>The 1D and 2D cloud probes (1D-C & 2D-C) were found to undercount particles in the smaller size channels due to reduced depths of field for these sizes<br>(continued on reverse) |                                     |   |

DD FORM 1473

EDITION OF 1 NOV 65 IS OBSOLETE

UNCLASSIFIED

SECURITY CLASSIFICATION OF THIS PAGE (When Data Entered)

UNCLASSIFIED

SECURITY CLASSIFICATION OF THIS PAGE(When Data Entered)

*100 m*. Actually the problem is both one of undercounting and missizing. An iterative correction scheme is necessary to truly account for both but would be too cumbersome, for real time use. A channel-by-channel correction scheme was found for the 1D-C probe (which is similar to that provided by PMS) and gives satisfactory corrections for many spectral shapes. Use of a constant depth of field was found to be best for the 2D-C probe. An artifact-rejection scheme for the 2D-C probe is discussed.

The phase discrimination option for the 2D-C probe was found to be  $\sim 25\%$  effective in detecting the ice phase in mixed cloud.

The PMS Axially Scattering Spectrometer Probe (ASSP) and Forward Scattering Spectrometer Probe (FSSP) artificially broaden droplet spectra, up to twice the standard deviation around the mean size measured by the cloud gun (CG), due to nonuniformities in beam intensities. Uncertainties in sample volume and losses during instrument dead times incur errors in droplet concentrations.

Comparisons were made between the ASSP, FSSP, CG and CSIRO liquid water device. The CG and FSSP compared well in droplet concentration while the ASSP indicated consistently lower values. The FSSP measured slightly larger droplet diameters than did either the ASSP or CG.

The liquid water content (LWC) comparisons indicated that the ASSP and FSSP-measured LWC's 2-3 times those of the CG; the FSSP values are typically 50% higher than the ASSP due to its larger measured droplet sizes. The CSIRO probe and ASSP were in good agreement although a fair amount of scatter existed in the data.

This report is a continuation of and supplement to work presented in our Scientific Report No. 1 under this contract.

UNCLASSIFIED

SECURITY CLASSIFICATION OF THIS PAGE(When Data Entered)

# TABLE OF CONTENTS

|  | <u>Page</u> |
|--|-------------|
| 1. Introduction . . . . .  | 1           |
| 2. Instruments Used in Evaluation Tests . . . . .  | 2           |
| a. Particle Measuring Systems (PMS) Axially Scattering Spectrometer Probe (ASSP) . . . . . | 2           |
| b. PMS Forward Scattering Spectrometer Probe (FSSP) . . . . .                              | 2           |
| c. PMS Optical Array Cloud Droplet Spectrometer Probe (1D-C) . . . . .                     | 2           |
| d. PMS 2D Optical Array Spectrometer Probe (2D-C) . . . . .                                | 2           |
| e. CSIRO Liquid Water Device (CSIRO) . . . . .   | 2           |
| 3. Procedure . . . . .   | 3           |
| 4. Results and Discussion . . . . .  | 6           |
| a. Studies of the Response of the 1D-C Probe . . . . .                                     | 6           |
| b. 2D-C Probe Studies . . . . .  | 22          |
| c. Studies of 2D-C Phase Discrimination . . . . .  | 27          |
| d. Cloud Gun, ASSP, FSSP and CSIRO Intercomparisons . . . . .                              | 31          |
| e. Study of the Response of the ASSP to Ice Particles . . . . .                            | 53          |
| 5. Summary and Conclusions . . . . .   | 55          |
| REFERENCES . . . . .   | 59          |
| APPENDIX A. Ice Crystal Collection and Photography . . . . .                               | 60          |
| APPENDIX B. The Cloud Gun . . . . .  | 64          |

|                    |                                     |
|--------------------|-------------------------------------|
| A copy for         |                                     |
| NTIS GRA&I         | <input checked="" type="checkbox"/> |
| DTIC TAB           | <input type="checkbox"/>            |
| Unannounced        | <input type="checkbox"/>            |
| Justification      |                                     |
| By _____           |                                     |
| Distribution/      |                                     |
| Availability Codes |                                     |
| Avail and/or       |                                     |
| Not Avail          |                                     |

A

## 1. Introduction

Recent years have seen rapid advances in the technology of airborne measurements of cloud hydrometeors. One impetus for these advances came from the development and marketing of a variety of electro-optical instruments by Particle Measuring Systems of Boulder, Colorado. Increasing availability and use of cloud physics aircraft provided additional motivation to the technological progress. As always, the use of new technologies for scientific studies requires a great deal of careful analysis of the new instruments. This need formed the basic motivation for the work described in this report.

The specific objectives of this work were defined at the outset to be the following:

- a. Compare bench determinations of ASSP\* and FSSP sample areas with those determined during actual cloud sampling.
- b. Evaluate the accuracy of the overlap in size range between the FSSP (or ASSP) and 1D-C (or 2D-C) probes.
- c. Evaluate the response of the ASSP and FSSP probes to ice crystals.
- d. These objectives were addressed under Contract No. F19629-79-C-0029 beginning in December, 1978, with a funding level of approximately \$79 K over 2 years.

The approach taken to this study was to conduct laboratory and field calibrations of selected instruments, the latter at the Elk Mountain Observatory. From these calibrations, the problem areas listed above were to be better understood and practical schemes were to be developed for the interpretation of data produced by the probes.

A preliminary report was written in October 1979 (Scientific Report No. 1, AFGL-TR-79-0251). This final report summarizes all of the work performed under subject contract although some details fully given in the Scientific Report will not be repeated.

\*See Section 2 for descriptions of instruments tested.

## 2. Instruments Used in Evaluation Tests

### a. Particle Measuring Systems (PMS) Axially Scattering Spectrometer Probe (ASSP)

Model: ASSP-100

History: This unit is on loan to us from the Water and Power Resources Service (WPRS, formerly the Bureau of Reclamation). The unit was refinished by PMS during the summer of 1978, and "strobe and activity" circuitry added in October 1978.

### b. PMS Forward Scattering Spectrometer Probe (FSSP)

Model: FSSP-100

History: In 1979 a unit was leased from PMS for the duration of the tests. The unit was used at PMS as a reference standard. For the 1980 tests a modified FSSP from the NCAR sailplane was loaned to us from the CSD at NCAR.

### c. PMS Optical Array Cloud Droplet Spectrometer Probe (1D-C)

Model: OAP-200X

History: The unit which was leased to us by PMS for the 1979 tests was calibrated by PMS to 20  $\mu\text{m}$  resolution on 7 March 1979. A different instrument was leased to us by PMS for the 1980 tests.

### d. PMS 2D Optical Array Spectrometer Probe (2D-C)

Model: OAP-2D-C

History: Two separate units were leased from PMS for the 1979 and 1980 tests. Both included the Phase Discrimination Option. The 1979 unit was calibrated on 7 March 1979, and the 1980 unit on 27 February 1980, both to 25  $\mu\text{m}$  bin widths.

### e. CSIRO Liquid Water Device (CSIRO)

History: This device was designed by Warren King of CSIRO. The one used in these studies was built at the University of Wyoming for use on the Queen-Air research aircraft

and is still considered to be in an experimental stage of development.

### 3. Procedure

The majority of our tests were performed at the Elk Mountain Observatory, which is operated by the Department of Atmospheric Science at the University of Wyoming. The Observatory is located near the summit (3.29 km MSL) of Elk Mountain, which is an isolated peak at the northernmost end of the Medicine Bow Range. The Elk Mountain summit is covered by clouds about one of every three days during the winter season.

For our tests the instruments were mounted in a wind tunnel that has a length of 8 m and a cross-sectional area of 20 cm x 43 cm. The wind tunnel is outdoors and rests diagonally along the stairway to an observation platform that is  $\sim 5$  m above ground level. The airspeed in the wind tunnel is  $22 \pm 4 \text{ m s}^{-1}$ . Soot-covered impactor slide samples (for droplet measurements) were taken from the observation platform near the mouth of the wind tunnel.

Data were collected primarily during periods when the Observatory was enveloped in clouds; specific tests were suited to periods where the clouds contained only ice crystals, but generally the cloud was of a mixed nature.

Droplet concentrations tended to be fairly low; usually around 200-300  $\text{cm}^{-3}$ , with mean diameters  $< 10 \text{ }\mu\text{m}$ . Pristine crystals formed in the orographic cloud and blowing snow from the surface were the most often observed ice particles. In these studies we have included blowing snow particles in our 2D-C and impactor slide analyses.

The data processing and recording systems were located inside the Observatory. The system is controlled by a Hewlett Packard mini-computer which allows for real time computation and display of certain meteorological parameters. Data are sampled once per second and stored on 1600 BPI magnetic tape.

A summary of the periods of field observations during 1979 and 1980 is contained in Tables 1 and 2.

TABLE 1 1978-79 SUMMARY  
OF FIELD TEST PERIODS

| DATE      | ASSP | FSSP | 1D-C | 2D-C | COMMENTS   |
|-----------|------|------|------|------|--|
| 12 Mar 79 |      |      |      |      | Installation of instruments                          |
| 13 Mar 79 | ✓    |      |      | ✓    | Study of effect of ice particles on ASSP spectrum    |
| 16 Mar 79 | ✓    |      | ✓    |      | Comparison of ASSP - 1D-C in overlap region          |
| 12 Mar 79 |      |      | ✓    | ✓    | Small ice particle studies                           |
| 25 Mar 79 | ✓    | ✓    |      |      | ASSP-FSSP intercomparison                            |
|           |      |      | ✓    | ✓    | Small ice particle studies                           |
|           | ✓    |      | ✓    |      | Comparison of ASSP-1D-C in overlap region            |
|           |      |      | ✓    |      | Glass bead calibrations in lab using mobile aperture |
| 2 Apr 79  |      |      |      | ✓    | Glass bead calibration in lab using mobile aperture  |
|           |      |      | ✓    | ✓    | Small ice particle studies                           |
|           |      |      | ✓    | ✓    | Mobile aperture affixed to 2D-C                      |
| 3 Apr 79  |      |      | ✓    | ✓    | Mobile aperture affixed to 2D-C                      |
|           |      |      | ✓    | ✓    | Mobile aperture affixed to 1D-C                      |
|           |      | ✓    |      | ✓    | Study of effect of ice on FSSP spectrum              |
|           |      |      | ✓    | ✓    | Small ice particle studies                           |
| 4 Apr 79  | ✓    |      | ✓    |      | Comparison of ASSP - 1D-C in overlap region          |

KEY: ASSP - PMS axially Scattering Spectrometer Probe  
 FSSP - DMS Forward Scattering Spectrometer Probe  
 1D-C - PMS 1D Optical Array Spectrometer Probe  
 2D-C - PMS 2D Optical Array Spectrometer Probe

TABLE 2

## 1980 SUMMARY OF FIELD TEST PERIODS

| Date      | ASSP | FSSP | 1D-C | 2D-C | Comments  |
|-----------|------|------|------|------|---|
| 15 Mar 80 | ✓    | ✓    |      |      | 2 CG comparisons<br>In cloud, no snow                         |
| 16 Mar 80 |      |      | ✓    | ✓    | 4 OH comparisons in cloud                                     |
| 19 Mar 80 | ✓    | ✓    |      |      | 8 CG comparisons  |
| 19 Mar 80 |      |      | ✓    | ✓    | In cloud and light snow<br>OH comparisons                     |
| 19 Mar 80 | ✓    |      |      | ✓    | In thin cloud - CG samples<br>blank ASSP ice response<br>test |
| 28 Mar 80 | (✓)  | ✓    |      |      | Many CG comparisons<br>ASSP laser intermittent                |

#### 4. Results and Discussion

##### a. Studies of the Response of the 1D-C Probe

The PMS 1D-C probe is an optical array device for sizing and counting cloud particles in the 20-300  $\mu\text{m}$  size range. As particles pass through a collimated laser beam they shadow a linear array of 15 diodes spaced 20  $\mu\text{m}$  apart. Particle size is deduced from the number of diodes shadowed. A 50% reduction in light flux reaching a diode is considered as shadowing and constitutes activation of that diode. Particles which shadow the end diodes are rejected.

One of the major uncertainties in the operation of this device is the depth of field (DOF) for particles  $\lesssim 100 \mu\text{m}$  diameter. Particles larger than this are detected and sized along the entire exposed length of the laser beam, but at smaller sizes the effective DOF decreases substantially. Bench tests were performed on the 1D-C probe in 1979 and 1980 to determine the response to particles which pass through different sections along the length of the laser beam. A movable aperture was designed and machined by Mr. P. Kelly of our department, which enabled samples to be introduced along any 1 cm segment of the sample aperture. A vacuum pump was attached to this aperture and airspeed were brought up to  $\sim 10 \text{ m s}^{-1}$ . Glass beads of calibrated sizes were used for these tests; bead sizes were checked by sizing under a microscope.

Using the movable aperture, the counting efficiency and sizing accuracy of the instrument were determined by comparing the size distributions indicated by the instrument for beads passing through different portions of the beam. For the determination of counting efficiency it was necessary to control the quantity of beads passed through the beam in each test. Even though this could not be done accurately without unduly complex procedures, the scatter in the data could be kept to reasonably low levels.

Figs. 1a and b show the mean diameter measured by the 1D-C probe as a function of sampling position along the beam. In general the indicated mean diameter increased slightly with distance away from the object plane. With the 100-110  $\mu\text{m}$  (106  $\mu\text{m}$  mean diameter) beads,

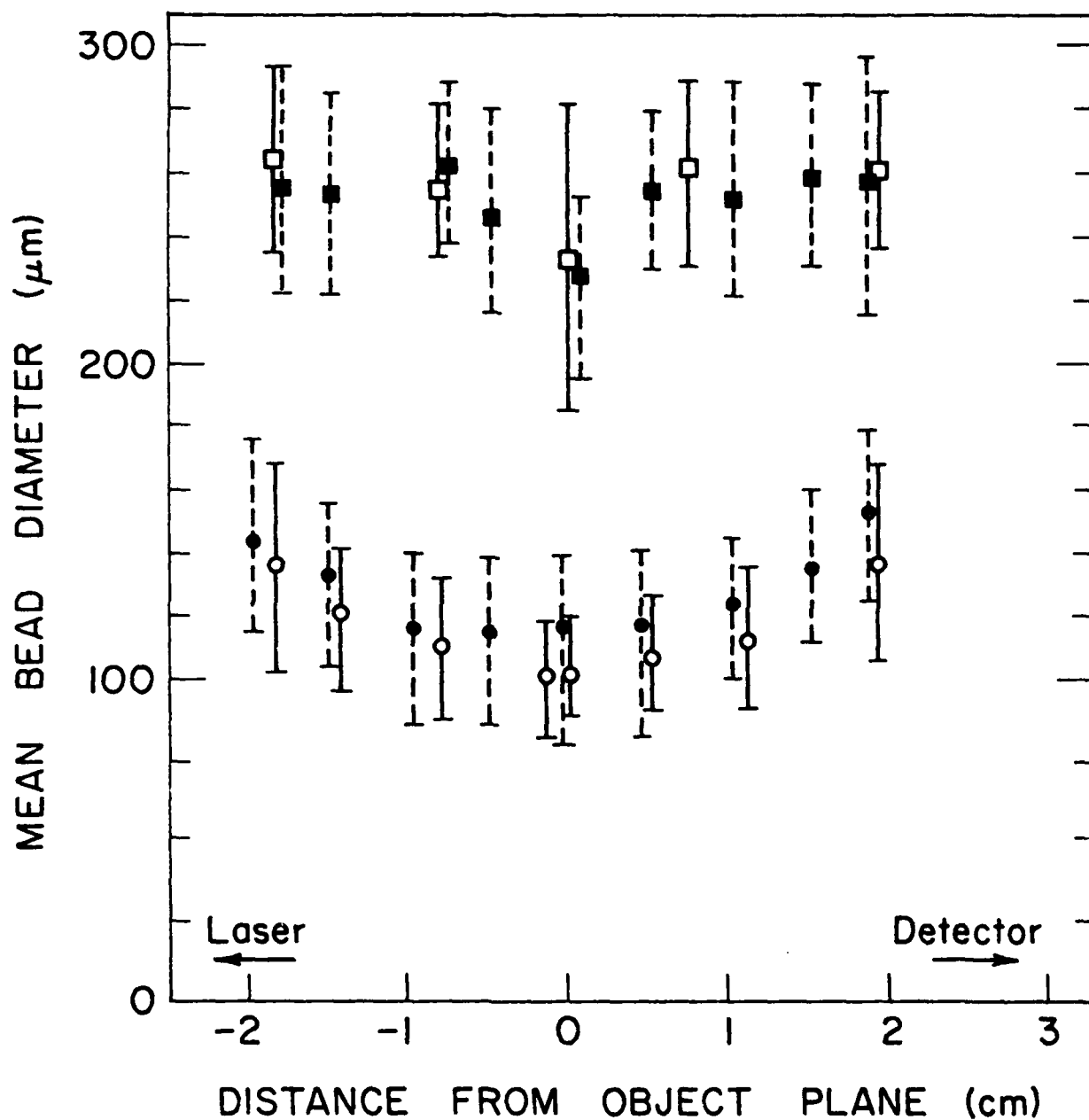


Fig. 1a Glass bead mean diameter measured by the 1D-C probe for different sampling positions. The vertical bars indicate one standard deviation from the mean. Symbols are as follows: (□) 1979 and (■) 1980 tests using 250-300 μm beads; (○) 1979 and (●) 1980 tests using 100-110 μm beads.

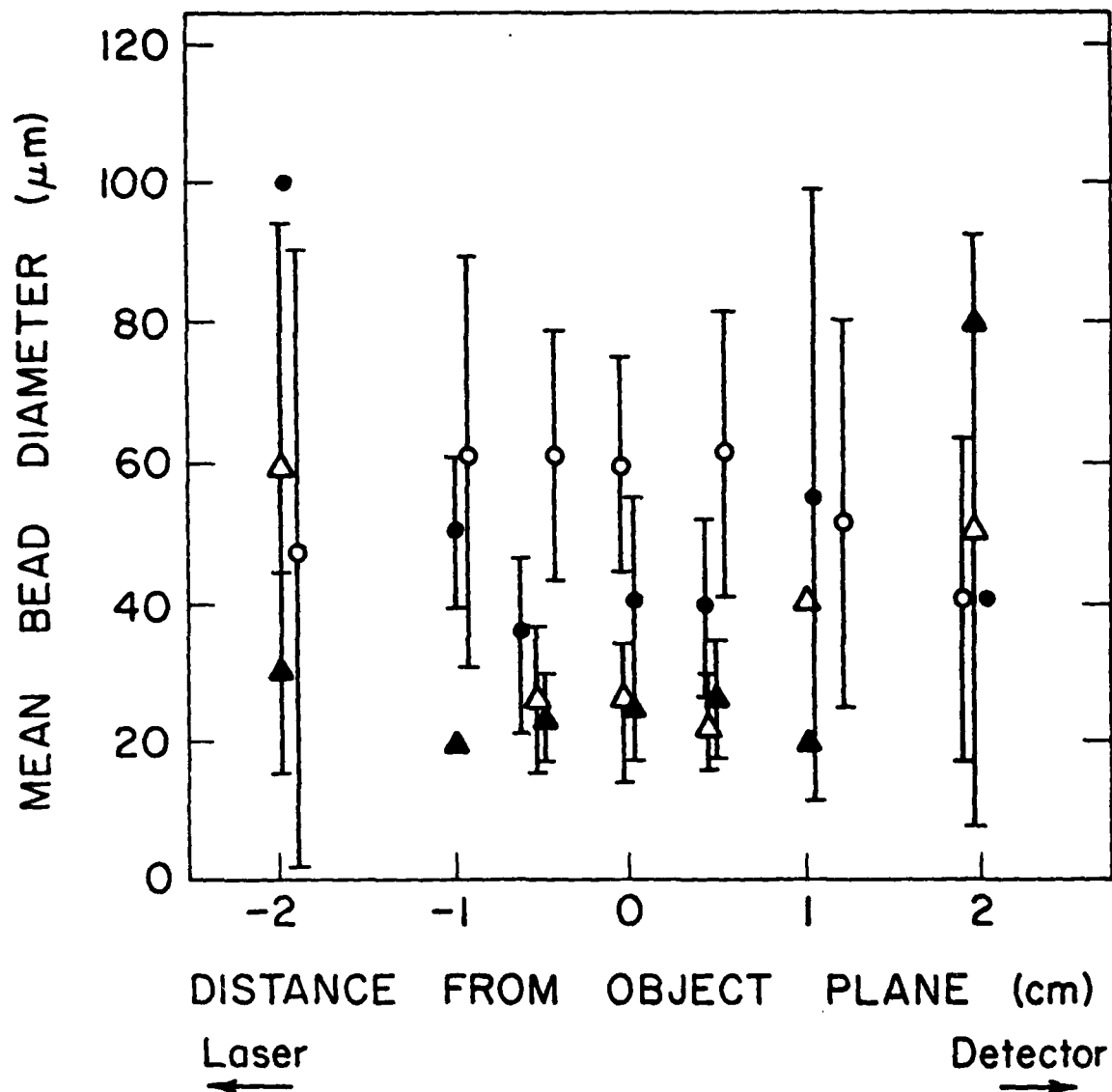


Fig. 1b Glass bead mean diameter and standard deviation measured from the 1D-C probe for 1980 tests using (▲) 15-25 μm, (△) 25-35 μm, (●) 35-45 μm, and (○) 45-75 μm beads. Points with no error bars indicate that counts were restricted to a single channel.

the results obtained in 1979 and in 1980 were similar even though different probes were used in the two tests. This reinforces the validity of the results. Fig. 2 shows the counting efficiencies of the two probes for this size range. The two data sets are not in good agreement in terms of counting efficiency, however, the 1980 data appear to be more consistent.

The measured mean diameters for beads in the 250-300  $\mu\text{m}$  (mean size 259  $\mu\text{m}$ ) range are nearly the same at all points across the aperture. The efficiency of counting these beads was also fairly constant along the beam length, within experimental uncertainty. As shown in Fig. 2, for beads of smaller sizes the counting efficiency drops off rapidly with distance from the object plane, as expected from depth of field calculations. Sizing at and near the object plane is reasonably accurate for the 40  $\mu\text{m}$  and 60  $\mu\text{m}$  beads. The difference between 20 and 30  $\mu\text{m}$  beads couldn't be resolved, due to the 20  $\mu\text{m}$  element size of the detector array. Beads of 6  $\mu\text{m}$  and 12  $\mu\text{m}$  sizes were not detected at all at any point along the sampling aperture.

Counting efficiencies for each channel were determined from the 1979 bead tests and presented in Scientific Report No. 1. These empirically determined values described the effect of missizing and undercounting of nearly monodisperse particles. These results showed that the counting efficiencies decreased substantially as the beads were sampled further from the object plane; the values for channels 2-5 were affected the most. Aperture tests conducted in the wind tunnel, where ice crystals and blowing snow were sampled, produced similar results. Counting efficiencies were higher than those from the glass bead tests yet they displayed the same general features across the size range of the probe. The values may have been higher in these tests which used fairly wide ice particle size distributions because of missizing; a size channel loses counts to its neighbors but similarly gains some of their missized particle counts.

Determination of a correction scheme to recover the "true" particle spectrum from that measured is a complex matter. There are

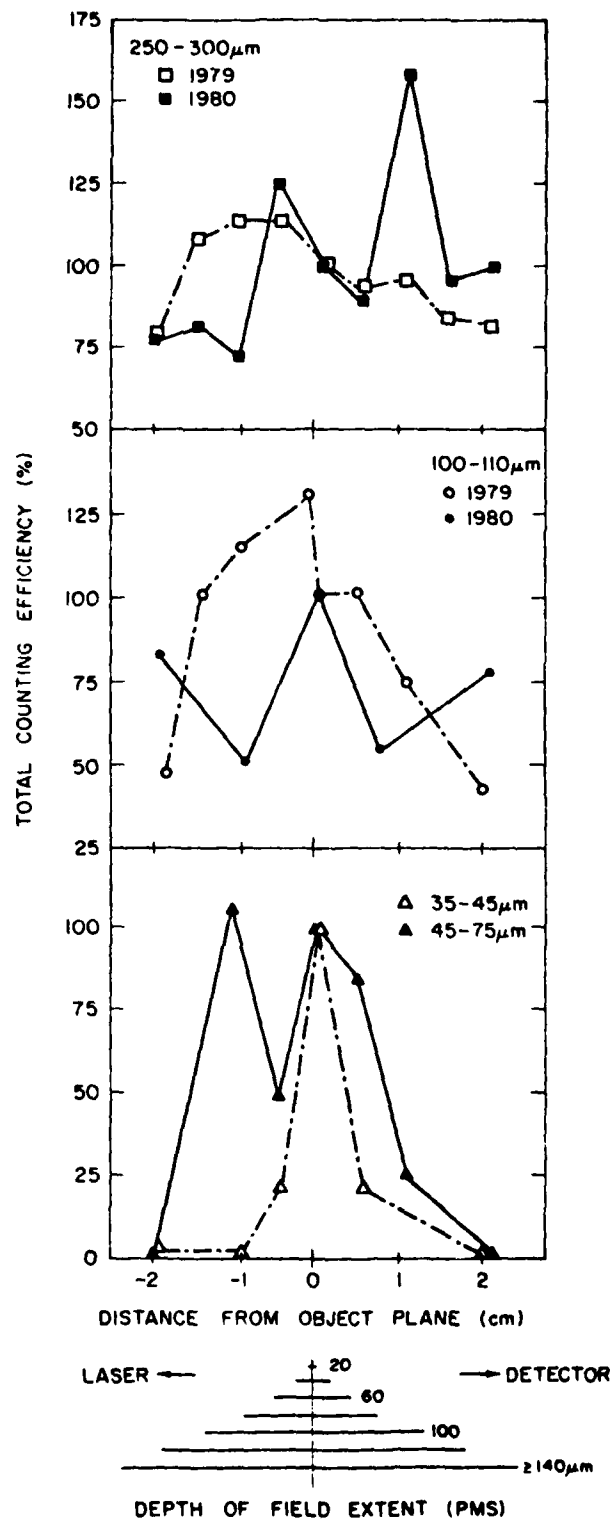


Fig. 2 Total counting efficiency of the 1D-C probe plotted against sampling position. The efficiency is defined as the ratio of glass beads detected away from the object plane to those detected at the object plane.

two interrelated problems to be accounted for: undercounting and mis-sizing. When particles are sampled at distances away from the object plane their shadows enlarge as they become more out of focus. At the same time the shadow becomes more diffuse and may not lead to sufficient light reduction to exceed the threshold level for diode shadowing. The data shown in Figs. 1a, 1b and 2 demonstrate these effects. An iterative correction scheme could be constructed on the basis of the bead tests, but such a scheme would be too cumbersome for operational use, and data quality from the bead tests would render the scheme insufficiently accurate.

As a result, a more pragmatic approach was followed: size distributions of polydispersed particle populations given by the 1D-C probe and by a direct sampling technique were compared. The direct-sampling technique used for reference is the O-H sampling technique; Appendix A contains a brief summary and evaluation of the method. While there are some limitations of accuracy for direct sampling also, these are relatively minor and the simplicity and directness of the method increases confidence in the results.

By comparing O-H data with 1D-C data for 11 samples in 1979 the counting efficiency as a function of particle size was found to be given by the curve shown in Fig. 3 (Fig. 20 of Scientific Report No. 1). The counting efficiency given here is an average for the complete sampling aperture, in contrast to that given in Fig. 2.

For comparison, the counting efficiencies (the fraction of total aperture width represented by the DOF for given channels) corresponding to the DOF figures given by PMS are also shown in Fig. 3. PMS supplies two sets of DOF values: one represents the reduced DOF's due to the small particle size, the other adds a "sample probability" which describes the probability that a particle in that channel will be sized correctly. We have derived correction factors for the 1979 tests and the PMS DOF's without sample probability; these factors are used to multiply particle concentrations in each channel to obtain the "true" spectrum. These are given in Table 3. The empirical data are not significantly different from those based on PMS' determinations of DOF.

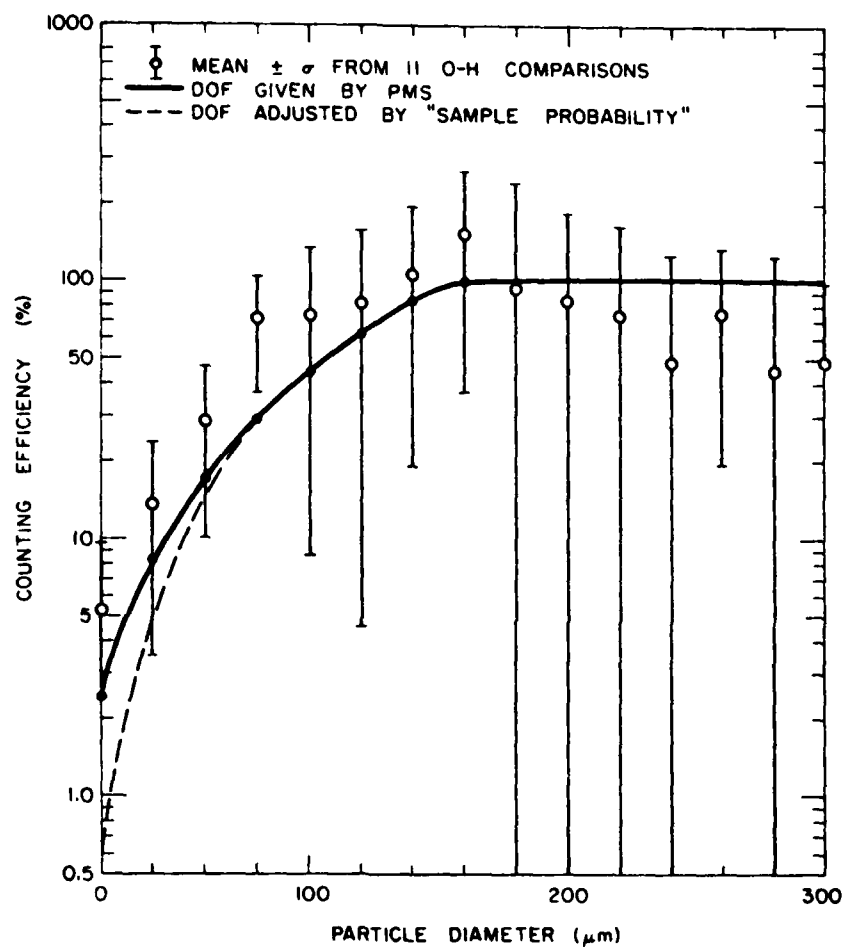


Fig. 3 Counting efficiency plotted against ice particle diameter for 1D-C data (o) and those predicted by PMS' depth of field values (— and - - -). 1D-C data is based on 11 O-H slide comparisons; means and standard deviations are shown. The data were collected at the Elk Mountain Observatory in 1979.

TABLE 3  
CORRECTION FACTORS FOR PARTICLES OF DIFFERENT SIZES

| Channel | Midpoint<br>( $\mu\text{m}$ ) | Correction Factor |                          | PMS<br>Sample<br>Probability | From<br>"Real"<br>DOF |
|---------|-------------------------------|-------------------|--------------------------|------------------------------|-----------------------|
|         |                               | Wyoming Tests     | From DOF<br>Given by PMS |                              |                       |
| 1       | 20                            | 23.5 $\pm$ 13.0   | 42.1                     | 26%                          | 162                   |
| 2       | 40                            | 11.3 $\pm$ 6.5    | 12.7                     | 62%                          | 20.5                  |
| 3       | 60                            | 5.5 $\pm$ 3.8     | 6.0                      | 89%                          | 6.7                   |
| 4       | 80                            | 1.7 $\pm$ 1.0     | 3.6                      | 100%                         | 3.6                   |
| 5       | 100                           | 2.1 $\pm$ 1.7     | 2.3                      | 100%                         |                       |
| 6       | 120                           | 1.5 $\pm$ 1.1     | 1.6                      |                              |                       |
| 7       | 140                           | 1.4 $\pm$ 1.5     | 1                        |                              |                       |
| 8       | 160                           | 0.56 $\pm$ 0.32   | 1                        |                              |                       |
| 9       | 180                           | 1.1 $\pm$ 0.75    | 1                        |                              |                       |
| 10      | 200                           | 1.6 $\pm$ 1.0     | 1                        |                              |                       |
| 11      | 220                           | 1.3 $\pm$ 0.69    | 1                        |                              |                       |
| 12      | 240                           | 2.7 $\pm$ 1.9     | 1                        |                              |                       |
| 13      | 260                           | 1.1 $\pm$ 0.53    | 1                        |                              |                       |
| 14      | 280                           | 3.2 $\pm$ 2.3     | 1                        |                              |                       |
| 15      | 300                           | 3.0 $\pm$ 2.0     | 1                        |                              |                       |

The correction factors given in Table 3 were derived from data collected in 1979. Since there is a dependence of the probe reaction to particle shape and to the form of the size distribution, the generality of the figures given in Table 3 is not immediately obvious. In order to examine the variations which may result from differences in sample characteristics, the correction factors of Table 3 were applied to an independent and different data set. One difference was that many of these size distributions had a broad peak at around 200  $\mu\text{m}$  instead of the exponential distributions encountered in 1979. Fig. 4 shows the raw and corrected size distributions for such a case. It is evident from this figure that the corrections in this case lead to excessively large numbers of particles in the lowest size channels. This is a result, it appears, of missizing of larger particles into these lower channels, and this error is magnified by the correction factors applied. In fact, for this type of distribution, the raw uncorrected data appear to give a closer representation of the real spectrum but indicate too low overall concentration. The corrected concentrations seem to be closer to the real value. These results point to the inadequacy of any correction scheme which doesn't account for missizing but merely corrects for each size range independently of the others.

Comparisons of number concentration and mean diameter measured by the 1D-C and O-H samples were performed using PMS' correction factors and those based on the 1979 comparisons. These are presented in Figs. 5 and 6. There doesn't appear to be a clear difference between the accuracies of the two correction schemes in predicting total particle concentrations. The mean particle sizes seem to be more accurate for the correction based on the Wyoming tests. Since the same results hold for the 1980 tests it can be concluded that these corrections can be applied with fair generality; however, the large amount of scatter remaining in this data show clearly the limitations of that conclusion, even beyond the shortcomings pointed out earlier in connection with Fig. 4.

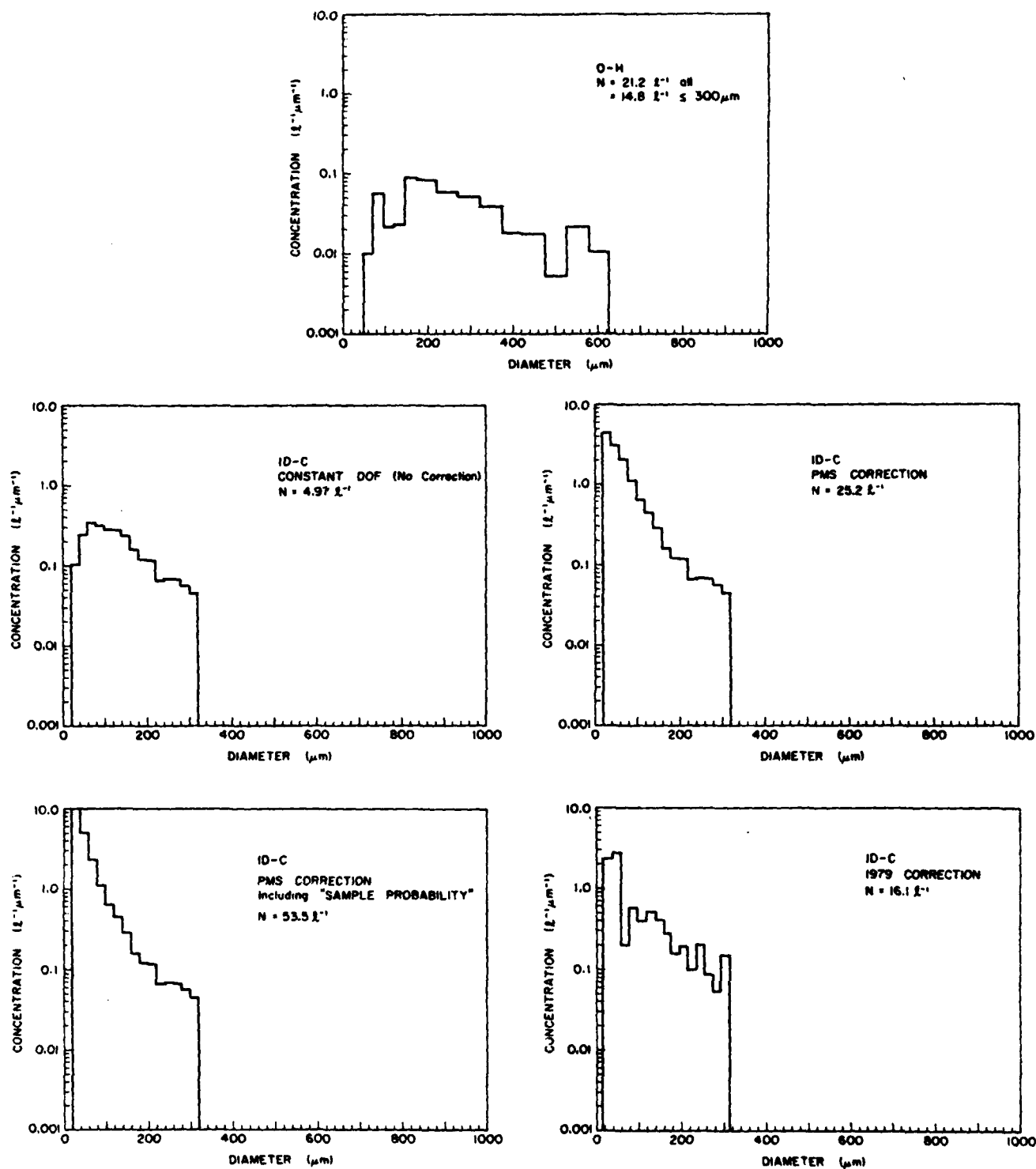


Fig. 4 Comparison of ice particle spectra measured in the wind tunnel at the Elk Mountain Observatory at 1131 MST, 16 March 1980. The O-H slide was exposed for 2 s. The ID-C data are 1 min averages around the O-H sample period.

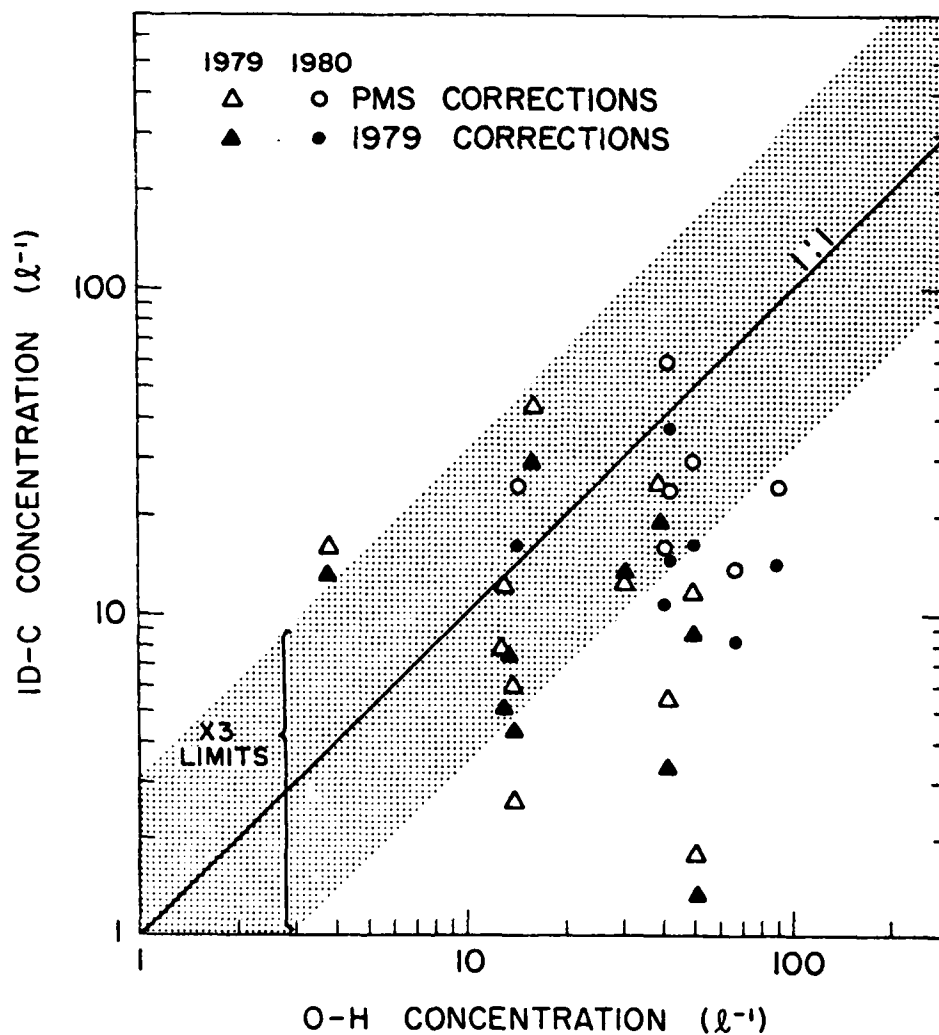


Fig. 5 Comparison of 0-H and 1D-C-measured ice particle concentrations using PMS' and our 1979 corrections. 0-H data are 2-10 s exposures. 1D-C data are 1 min samples around the 0-H sample period.

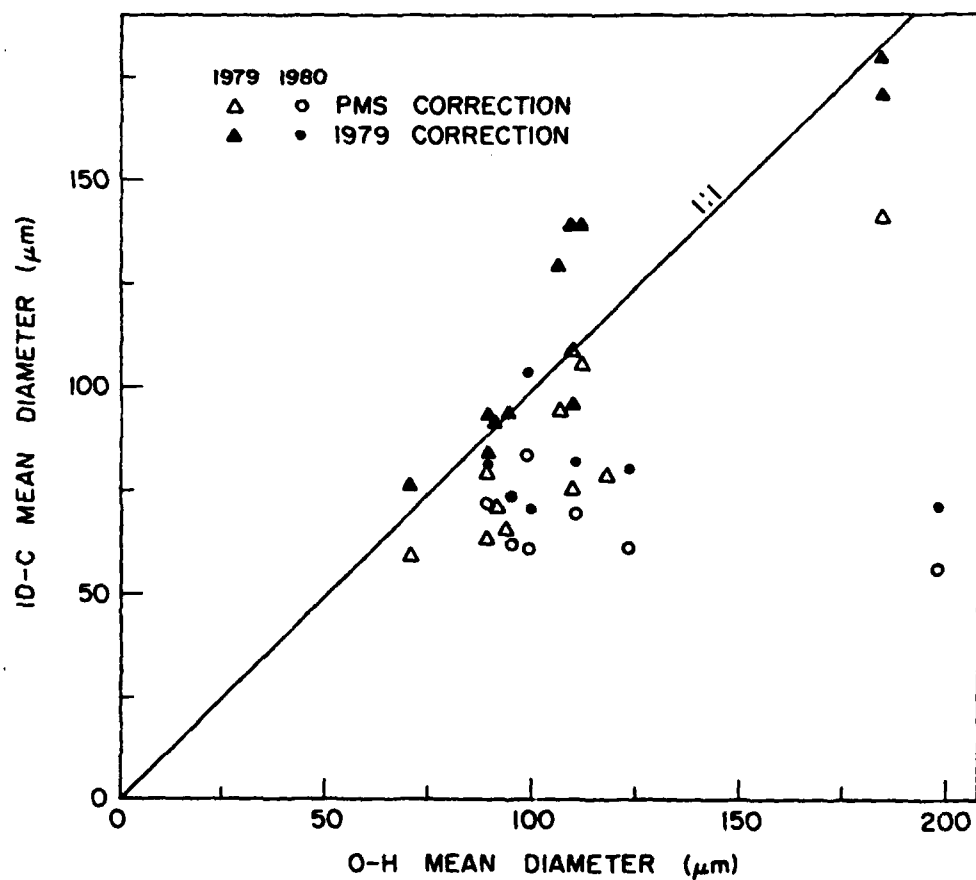


Fig. 6 Comparison of ice particle mean diameters from O-H slides and the ID-C probe. Samples are the same as those in Fig. 5.

To provide a further basis for assessing the accuracy of the 1D-C data, comparisons were made against a 2D-C probe. Previous comparisons and those to be given in the following section of this report revealed good agreement between O-H sample data and 2D-C data (used without corrections for reduced DOF for small particles). Thus there is justification for accepting 2D-C data as a basis for judging the less well-tested 1D-C data.

For these comparisons 30-sec averages of data were used. The two instruments were mounted alongside each other in the wind tunnel (the 2D-C probe will be discussed in the next section). Only particles with diameters to 300  $\mu\text{m}$  were included in these comparisons.

The results shown in Figs. 7 and 8 reveal substantial disagreements which were just barely hinted at by the fewer points available in Figs. 5 and 6. Using PMS' correction factors the underestimation of concentration by the 1D-C probe is less, but the size estimate is further off than for the Wyoming tests. This is a direct result of the larger correction factors given by PMS for the smallest particle sizes. The relatively small scatter of points in Figs. 7 and 8 attest to the consistency of the probes and of the analysis scheme for particle populations of a given character. Unfortunately this is the only data set of this kind available at the present.

A report by Knollenberg (1975) addressed the problem of the response of the 1D-C to various ice particle shapes. The probe tends to undersize most ice crystal habits due to their irregular shapes, whereas the probe sizing calibration was designed for spherically-shaped droplets. Both theoretical calculations and bench tests were used to determine relations between measured and actual size for various crystal shapes.

In the Scientific Report No. 1 several comparisons of spectra were presented to illustrate that use of the corrections helps improve agreement between the 1D-C measured spectra and 2D-C or O-H measured spectra, especially in the larger size ranges. An example (from 1979) which illustrates this point shown in Fig. 9 (Fig. 28 of Scientific Report No. 1).

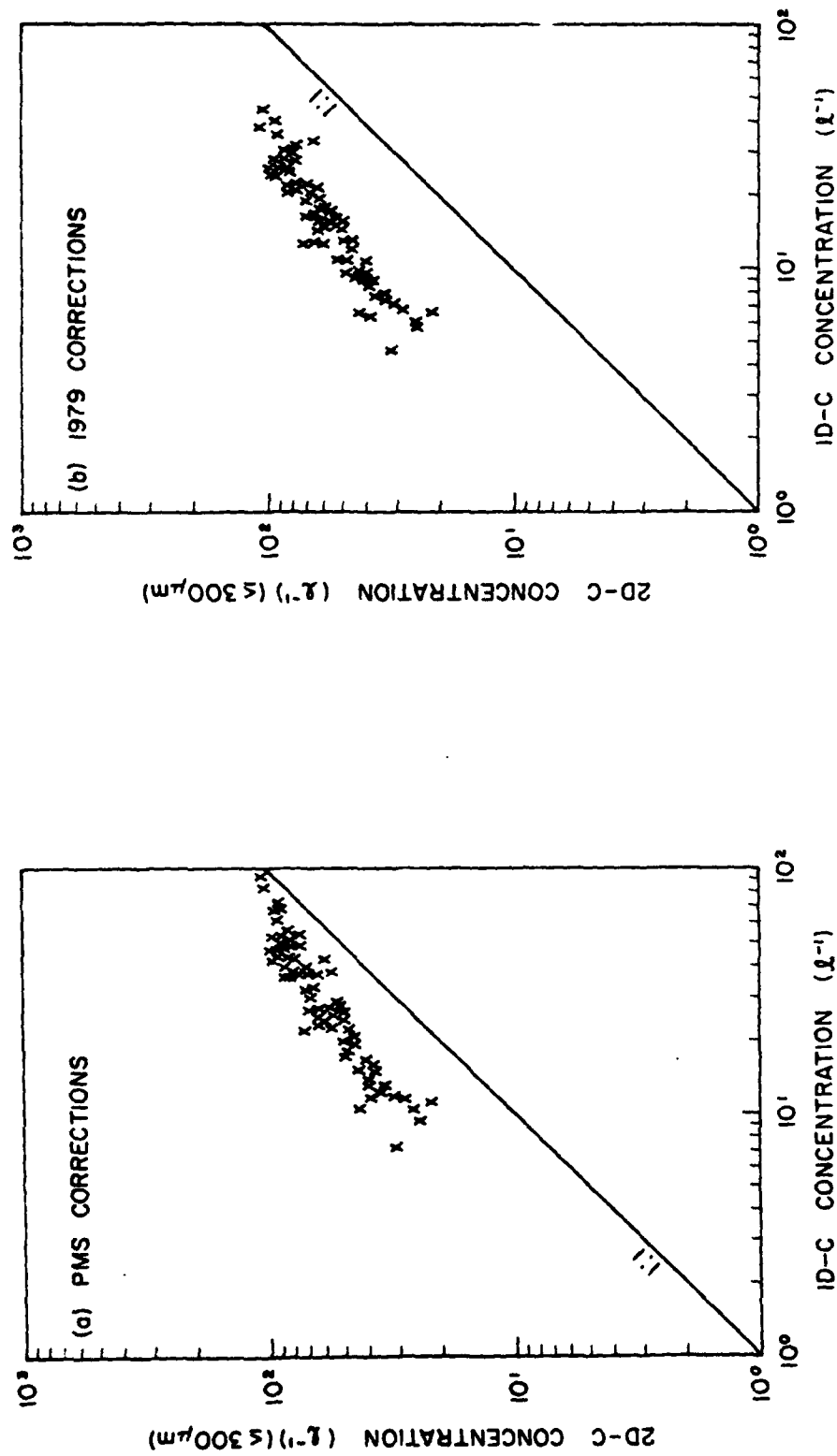


Fig. 7 Comparison of ice particle concentrations measured from the 1D-C and 2D-C probes. a) PMS corrections used for 1D-C data; b) 1979 corrections. Data are 30 s averages taken on 19 March 1980 at the Elk Mountain Observatory. A constant depth of field was used to analyze the 2D-C data and only particles with diameters  $< 300 \mu m$  were counted.

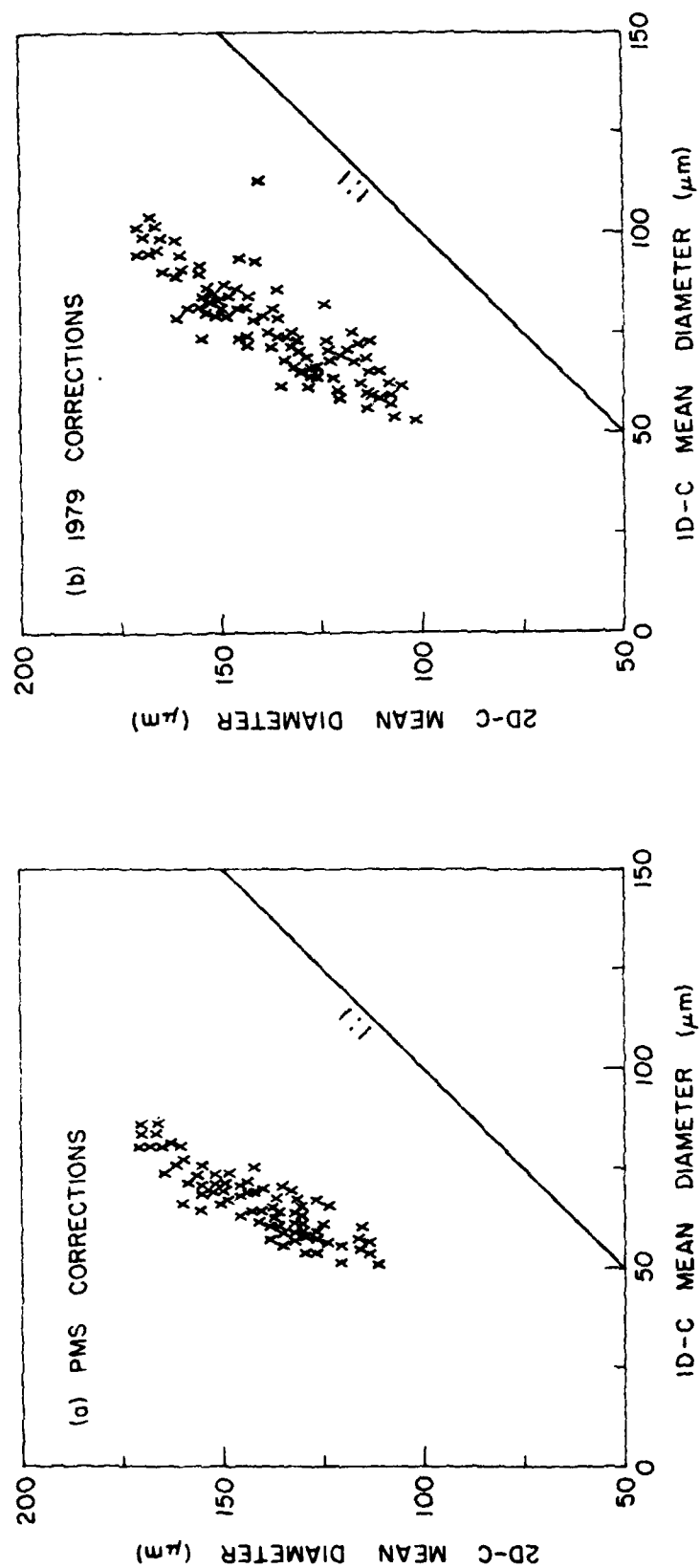


Fig. 8 Comparison of ice crystal mean diameters measured from the 1D-C and 2D-C probes. a) PMS corrections used for 1D-C data analysis; b) 1979 corrections used. Data are from the same sample described in Fig. 7.

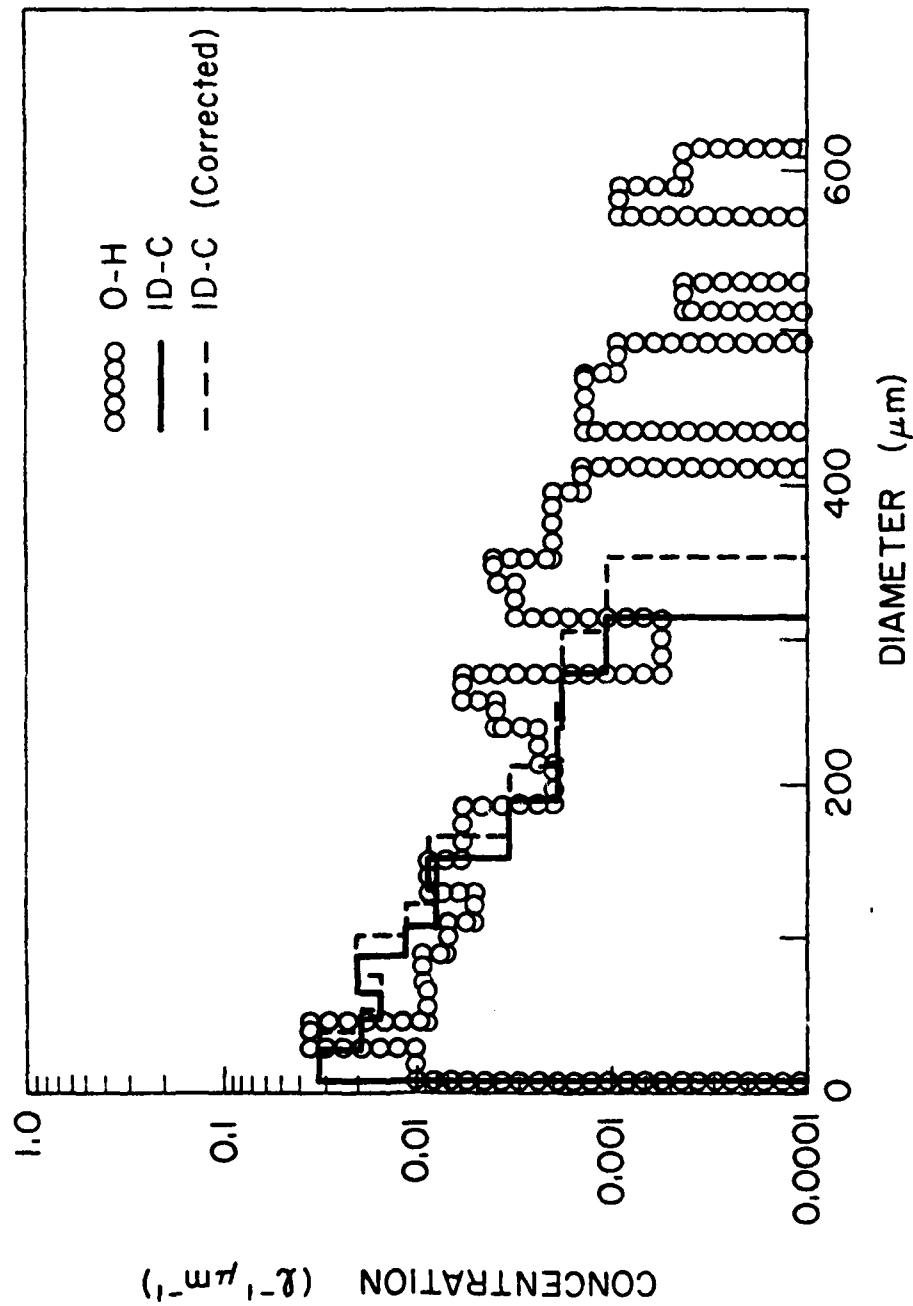


Fig. 9 Concentration plotted against ice particle diameter for data collected at the Elk Mountain Observatory at 1020 MST on 17 March 1979. ID-C data uncorrected (—) and corrected (---) for "irregular snow" (Knollenberg, 1975), and corresponding O-H data (○○○○) are shown. The O-H slide was exposed for 10 s; the ID-C data are a 1 min average taken around the O-H exposure time.

These corrections expand the measured spectra and in the cases shown produce better agreement with "true" spectra. However, the corrections correct only for mis-sizing and not undercounting which may occur for out-of-focus particles.

b. 2D-C Probe Studies

The PMS 2D-C probe is very similar to the 1D-C probe in its fundamentals. However, by sampling the on/off state of each element of the detector array at speeds matched to the particle velocity, the shadow image is recorded rather than just the maximum size as in the 1D-C probe. Other differences exist in optical path, and in the use of 25  $\mu\text{m}$  element spacing rather than 20  $\mu\text{m}$ .

The main advantage of the 2D-C probe is in the information content of particle shape. However, in these tests only the maximum indicated size of particles was evaluated.

One benefit of particle shape information is that "artifacts" can be recognized. The data used in this report have been corrected by removing artifacts according to the following criteria:

(1) For all images:

(a) If time between images is less than 1000 probe cycles, the particle is rejected. This corresponds to  $\sim 1/1000$  second of real time. With an air tunnel speed of  $2450 \text{ cm s}^{-1}$ , the 2D-C probe samples  $1.18 \text{ s}^{-1}$ . Sampling 1000 particles per second corresponds to 850 particles per liter which is higher than concentrations we have observed at Elk Mountain. The threshold of  $1/1000 \text{ s}$  was somewhat arbitrary; it could be reduced but appears to work well as is.

(b) If a rectangular box enclosing the image has an aspect ratio greater than 3:1 it is rejected. This is designed to catch "streakers", that is, liquid water shedding from the probe tips. It is assumed that the fraction of columns and needles passing the probe with C-axes parallel to the flight path will be low.

(c) If the image occupies less than 3% of a rectangular box enclosing it, it is rejected.

(d) If the image length is greater than 10 times the image width (perpendicular to the flight path) it is rejected. Again, this is designed to catch "streakers".

(2) If the image touches both sides of sample area on at least one scan it is assumed to be good.

For the samples used in O-H slide comparisons which will be described later, "artifacts" ranged from 33-52% of the total particle count, usually  $\sim 40\%$ . This is higher than the ratios normally encountered and may be due to the low airspeeds in the wind tunnel (minimum airspeed for the 2D-C used was  $24.5 \text{ m s}^{-1}$ ).

The dependence of 2D-C probe response on position along the sampling aperture was tested in a manner similar to the tests described for the 1D-C probe. These tests have been already fully detailed in Scientific Report No. 1, so they will not be repeated here. As position from the center of the sampling aperture increased, beads of  $106 \text{ }\mu\text{m}$  were sized up to  $125 \text{ }\mu\text{m}$  while  $260 \text{ }\mu\text{m}$  beads were sized fairly consistently along the entire aperture length. Counting efficiencies dropped off significantly with distance from the aperture center as well for the smaller beads. The conclusion drawn from those tests was that the best estimate for the size distribution resulted from using the data without any correction factors, even though slight oversizing and undercounting could clearly be demonstrated from particles sampled near the ends of the sampling aperture. Figures 10 and 11 demonstrate this point by comparing data derived from the probes with O-H sample data. Additional points from 1980 tests are included in these figures. Without correction factors the concentrations show better agreement than if a correction is applied based on PMS' values for DOF. The data for mean sizes are less clear: while for  $< 100 \text{ }\mu\text{m}$  mean sizes the corrected values give better agreement, for larger mean sizes the corrections would lead to serious underestimation.

The advisability of using uncorrected 2D-C data is also consistent with experience gathered under a large range of sampling conditions. Fig. 12 shows a comparison based on several data sources: several years of studies at the Elk Mountain Observatory, aircraft observations in Elk Mountain cap clouds, and data taken from aircraft in clouds over Spain.

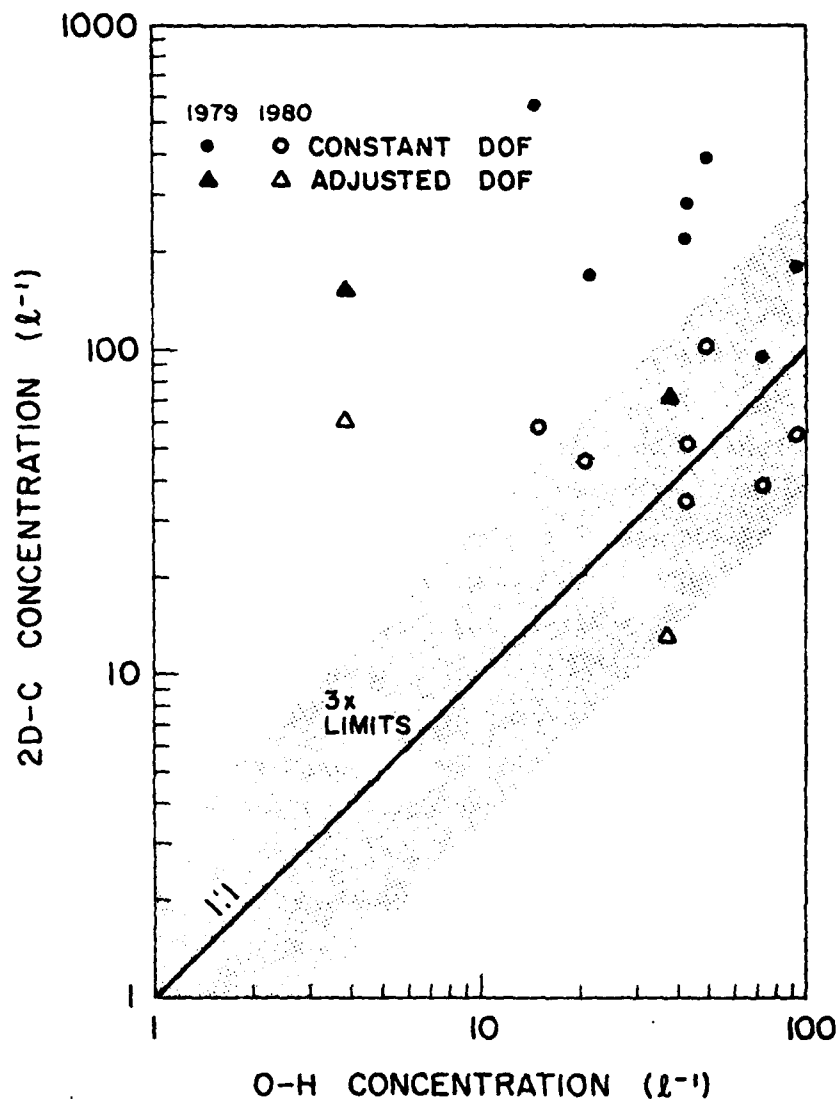


Fig. 10 Comparison of ice crystal concentrations measured from O-H slides and the 2D-C probe. O-H slides were exposed for 2-10 s, the corresponding 2D-C measurements represent a 1 min average around the O-H sample period. Data are from the Elk Mountain Observatory.

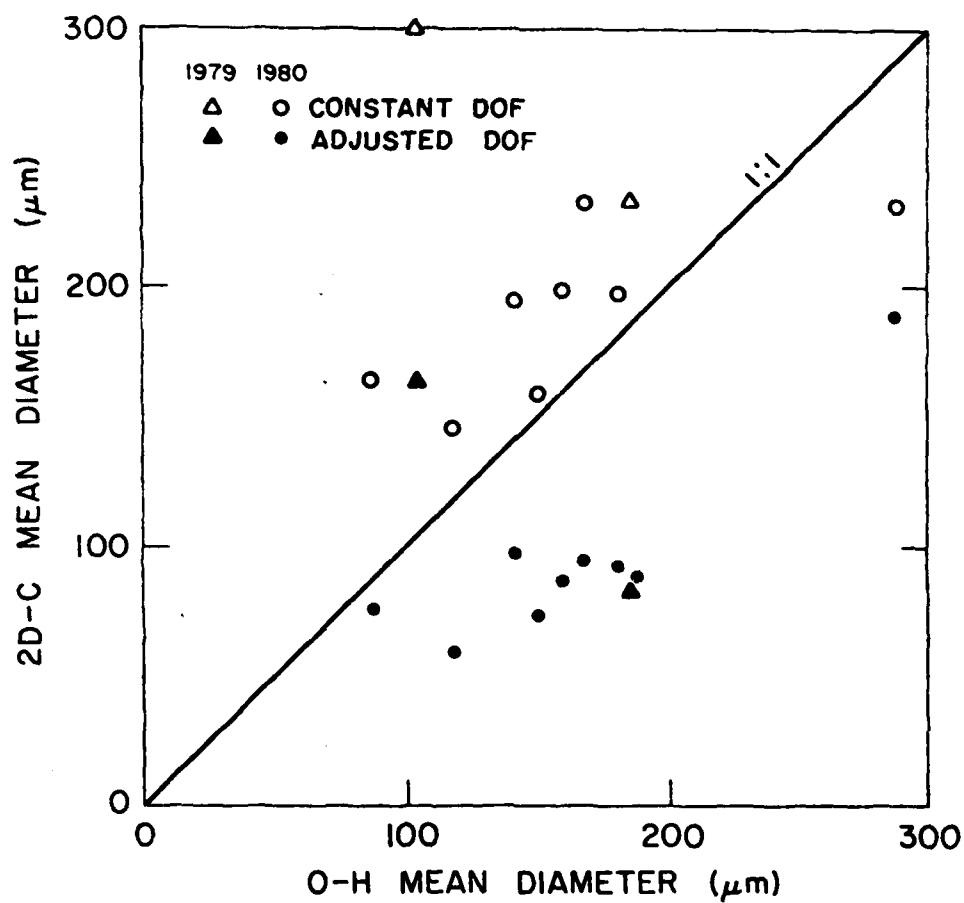


Fig. 11 Comparison of ice particle mean diameter measured by O-H slides and the 2D-C probe. Samples are described in the caption for Fig. 9.

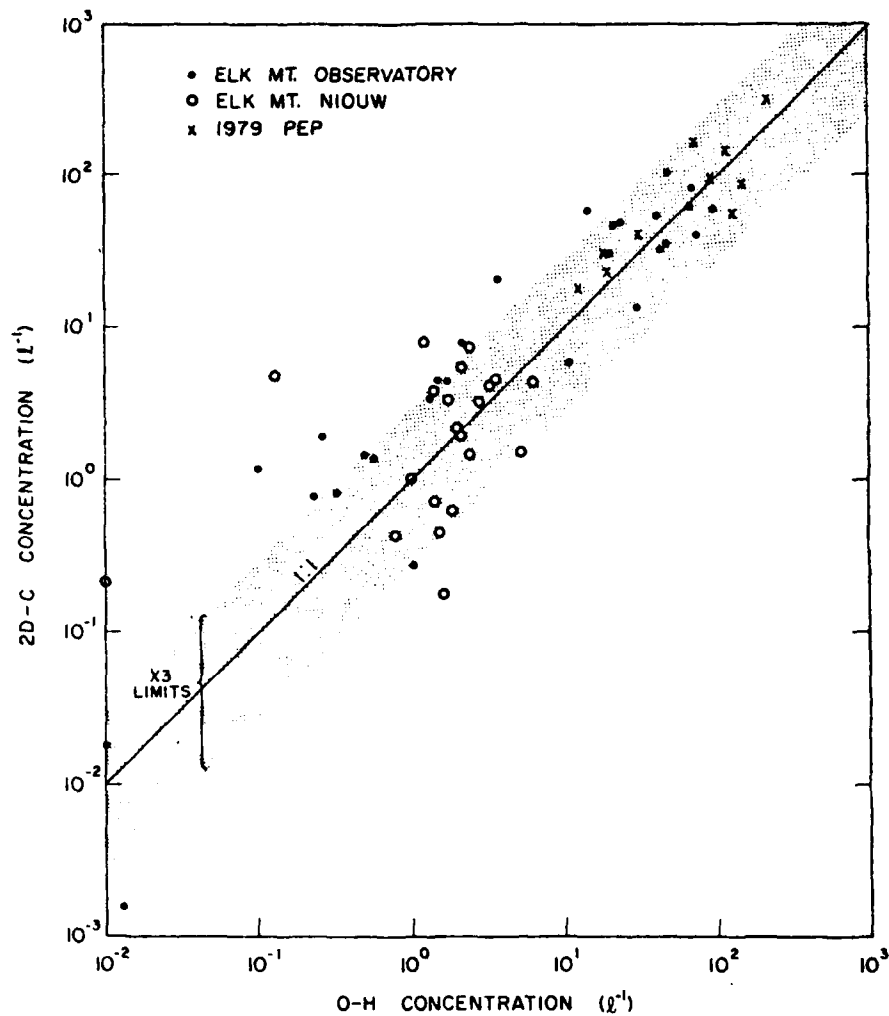


Fig. 12 Comparison of ice particle concentrations measured from O-H slides and the 2D-C probe. O-H samples were 2-30 s exposures, the corresponding 2D-C data from the aircraft covered the same time period and from Observatory 2D-C data represent a 1 min average around the O-H sample time.

The 2D-C data were analyzed in the same manner as described previously for the work under this project. Most of the data agree within a factor of three, which we consider acceptable. The spectra shown in Fig. 13 further illustrate the difference the smaller DOF's given by PMS make in the lower channels of the size distribution. Other such comparisons were presented in Scientific Report No. 1.

c. Studies of 2D-C Phase Discrimination

The 2D-C probes which were used for our studies had a phase discrimination feature designed to provide a method by which ice particles can be distinguished from large water droplets.

The laser used in the 2D-C probe is polarized such that the plane of polarization lies in the plane defined by laser, lenses, mirrors and photodetectors. The bi-refrigent property of ice particles results in depolarization of the laser beam. A beam-splitting Thompson prism allows light in the original plane of polarization to pass through yet diverts any light in an orthogonal plane of polarization. This diverted light is detected and classified into eight levels using a pulse height detector.

The response of the depolarization signal was checked during a 30 minute time period from 2205 to 2236 on 4 April 1979. During this time there were fluctuations in ice particle concentration but crystal sizes and habits remained nearly the same (see Table 4). The crystal habits were dendrites and blowing snow. There were no large water drops present.

One minute segments of data were averaged at five minute intervals to produce the results presented in Table 4 and Fig. 14. Table 4 contains information on 2D-C-measured total ice particle concentrations and sizes as well as those which produced a depolarized signal. Also included are the percentages of ice particles yielding given depolarization levels. The percentage of depolarizing particles is plotted against their measured size in Fig. 14. On the whole, the total percentage of depolarized particles remains near 20%, the value reported by PMS. This ratio is ~25% for particles  $\leq 100 \mu\text{m}$  in diameter, and decreases slowly to remain near 10% for particles  $\geq 500 \mu\text{m}$  in diameter.

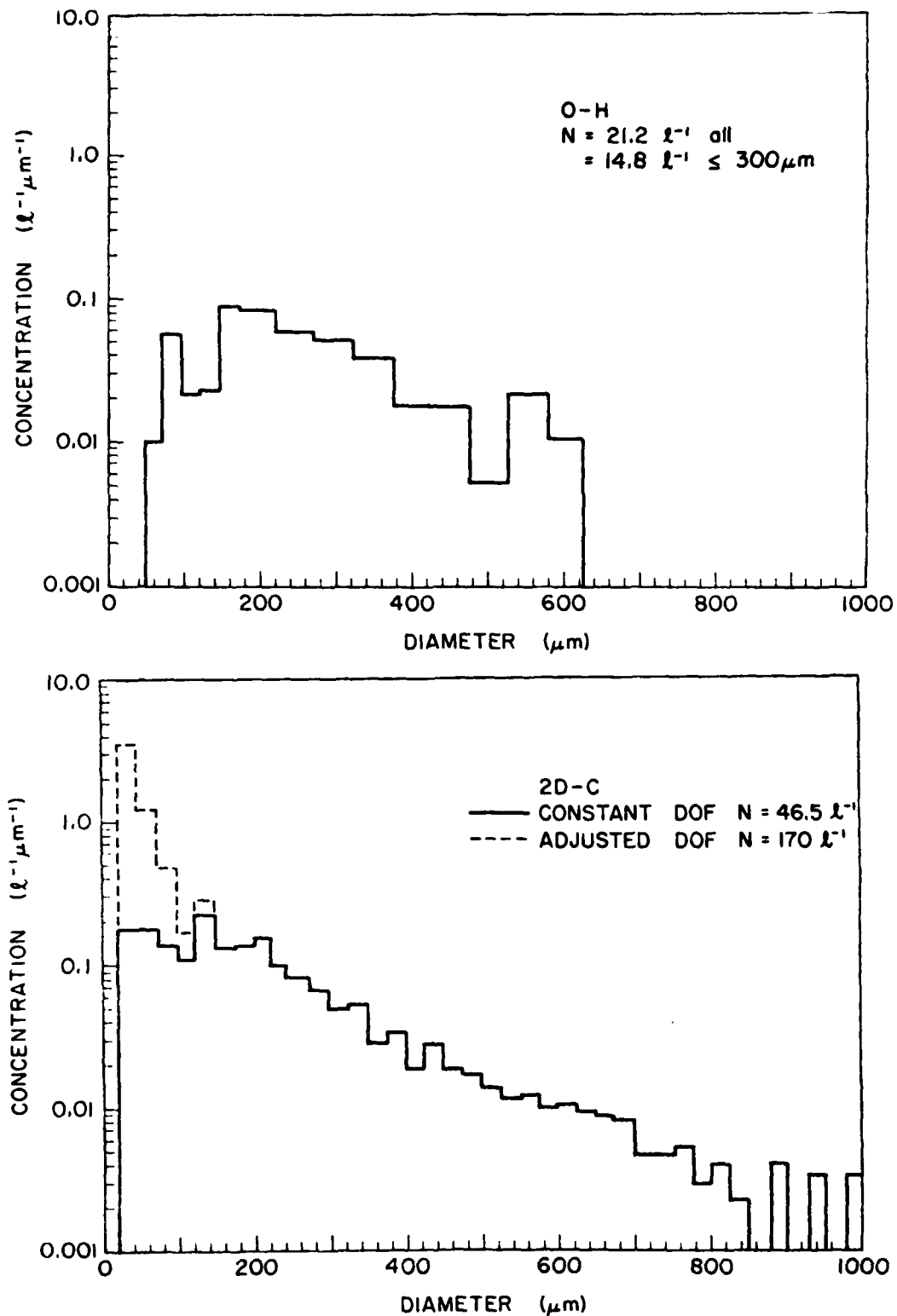


Fig. 13 Comparison of ice particle spectra measured from an O-H slide and the 2D-C probe. These spectra were taken during the same time period as those in Fig. 4.

TABLE 4

SUMMARY OF 2D-C DEPOLARIZATION STUDY  
4 APRIL 1979

| Time (MDT) | $N(l^{-1})$ |       |         | $d(\mu m)$ |       |                | $\sigma(\mu m)$ |       |                     |
|------------|-------------|-------|---------|------------|-------|----------------|-----------------|-------|---------------------|
|            | all         | depol | % depol | all        | depol | $\Delta_d(\%)$ | all             | depol | $\Delta_\sigma(\%)$ |
| 2205-2206  | 57          | 12    | 21.7    | 287        | 229   | -20.3          | 157             | 124   | -20.8               |
| 2210-2211  | 21          | 4.6   | 22.1    | 262        | 202   | -22.8          | 206             | 104   | -49.5               |
| 2215-2216  | 9.1         | 2.0   | 20.0    | 302        | 222   | -26.3          | 314             | 108   | -65.7               |
| 2220-2221  | 9.8         | 2.1   | 21.9    | 282        | 224   | -20.6          | 231             | 112   | -51.8               |
| 2225-2226  | 4.1         | 0.62  | 15.3    | 271        | 206   | -23.9          | 138             | 116   | -16.3               |
| 2230-2231  | 0.96        | 0.16  | 17.0    | 237        | 206   | -13.0          | 93              | 115   | +24.2               |
| 2235-2236  | 3.2         | 0.59  | 18.4    | 264        | 220   | -16.3          | 143             | 148   | + 3.3               |
| Average    |             |       | 19.5    |            |       | -18.7          |                 |       | -25.7               |

% Particles Per Depolarization Level

| Time (MDT) | 0    | 1   | 2   | 4   | 8   | 16  | 32 | 64   | 128 |
|------------|------|-----|-----|-----|-----|-----|----|------|-----|
| 2205-2206  | 78.6 | 5.2 | 7.6 | 5.7 | 2.7 | 0.2 | 0  | 0.1  | 0   |
| 2210-2211  | 77.6 | 4.4 | 7.6 | 7.2 | 3.0 | 0.2 | 0  | 0.04 | 0   |
| 2215-2216  | 78.1 | 4.3 | 7.0 | 6.5 | 3.6 | 0.5 | 0  | 0    | 0   |
| 2220-2221  | 76.9 | 4.4 | 6.8 | 7.7 | 3.7 | 0.5 | 0  | 0    | 0   |
| 2225-2226  | 83.9 | 4.7 | 5.9 | 4.4 | 1.0 | 0.1 | 0  | 0    | 0   |
| 2230-2231  | 84.7 | 4.3 | 5.8 | 3.6 | 1.5 | 0   | 0  | 0.1  | 0   |
| 2235-2236  | 83.8 | 4.1 | 5.2 | 4.8 | 2.1 | 0   | 0  | 0    | 0   |
| Average    | 80.5 | 4.5 | 6.6 | 5.7 | 2.5 | 0.2 | 0  | 0.03 | 0   |

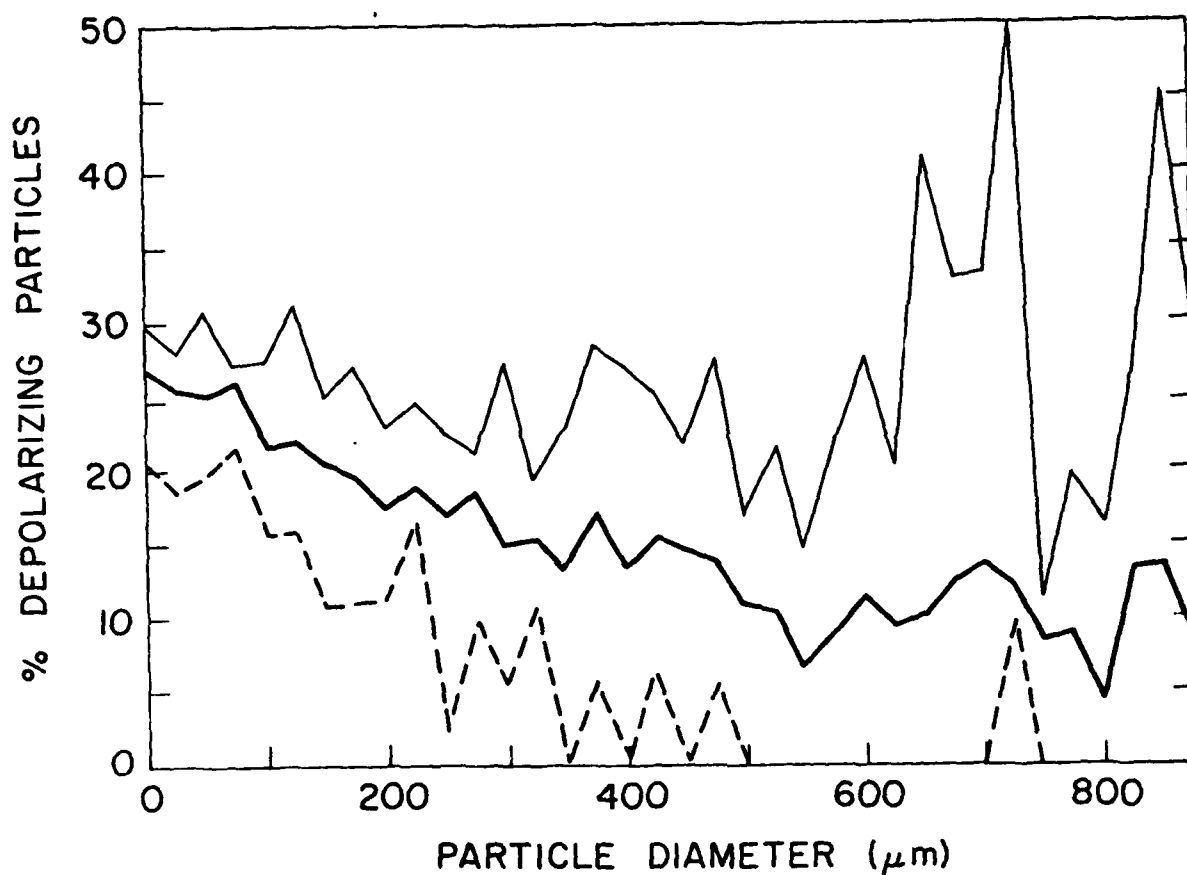


Fig. 14 Percentage of particles which produced a depolarizing signal to the 2D-C probe plotted against their size. The dark solid line is the mean of 7 min of probe data; the light solid line and the dashed line represent  $\pm$  one standard deviation from the mean.

These results do not completely describe the characteristics of the depolarization detector. The dependence of performance characteristics on crystal type was not examined in the tests reported here. Other work (by R. Hobbs of this Department) produced much more detailed information from independent data sets. The findings reported in Fig. 13 and Table 4 agree with the more detailed data sets.

d. Cloud Gun ASSP, FSSP and CSIRO Intercomparisons

The 1979 evaluations of the ASSP, (cf., Scientific Report No. 1) consisting mainly of cloud gun impactor samples, were influenced by the interaction of the airflow at the sampling aperture of the cloud gun (CG). Recognition of this problem led to the design and construction of an improved sampling intake of the cloud gun. Further information on the cloud gun is found in Appendix B.

Comparisons in 1980 emphasized evaluation of the FSSP probe in relation to the redesigned cloud gun. Additional data were also recorded comparing the FSSP to the ASSP and CSIRO.

(1) Spectral Comparisons

In 1979 the cloud gun measured droplet concentrations were  $\sim 2.3$  times greater than those measured by the ASSP as seen in Fig. 15, which is a comparison between the droplet concentration measured by the cloud gun and those measured by the ASSP and FSSP. During the 1980 season, although the number of samples is small, the cloud gun measured concentrations are seen to be only 1.3 times those measured by the ASSP. The agreement between the FSSP and CG-measured concentrations shown in Fig. 16 is excellent with very little scatter. The correlations coefficient between the two instruments is  $r = 0.88$ .

The mean droplet diameters as measured by the CG and ASSP/FSSP are compared in Fig. 17 & 18. The 1979 comparisons, seen in Fig. 17, show the

---

Note: The regression lines drawn through the concentration and liquid water data use the method of minimizing the least square error of the perpendicular distance from each point to the best-fit line. The regression is also forced through the origin as this represents the physical reality that when there are no droplets the measured concentrations and liquid water contents from both instruments should be zero.

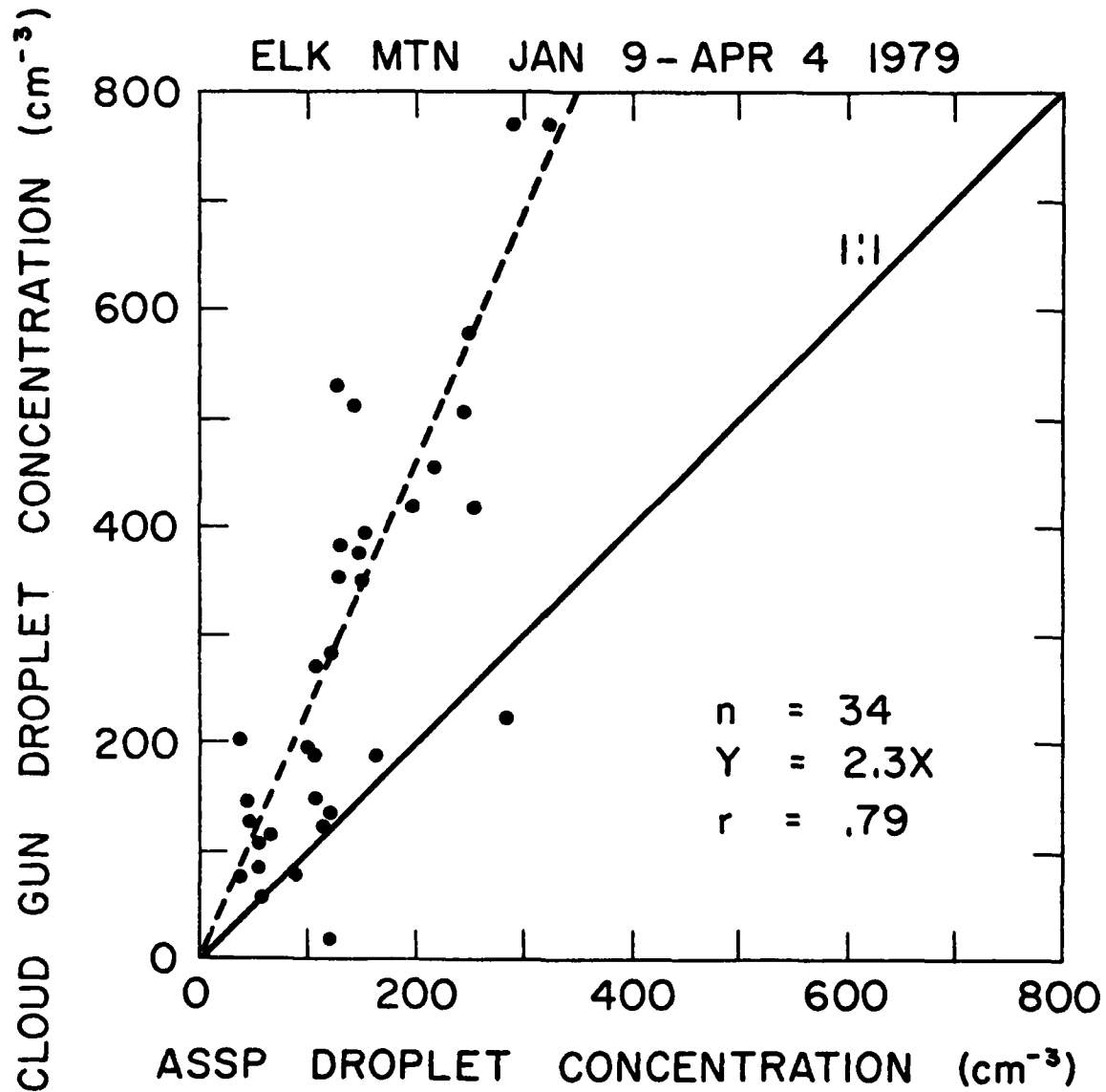


Fig. 15 Comparison of ASSP and cloud gun droplet concentrations measured during the 1979 field season.

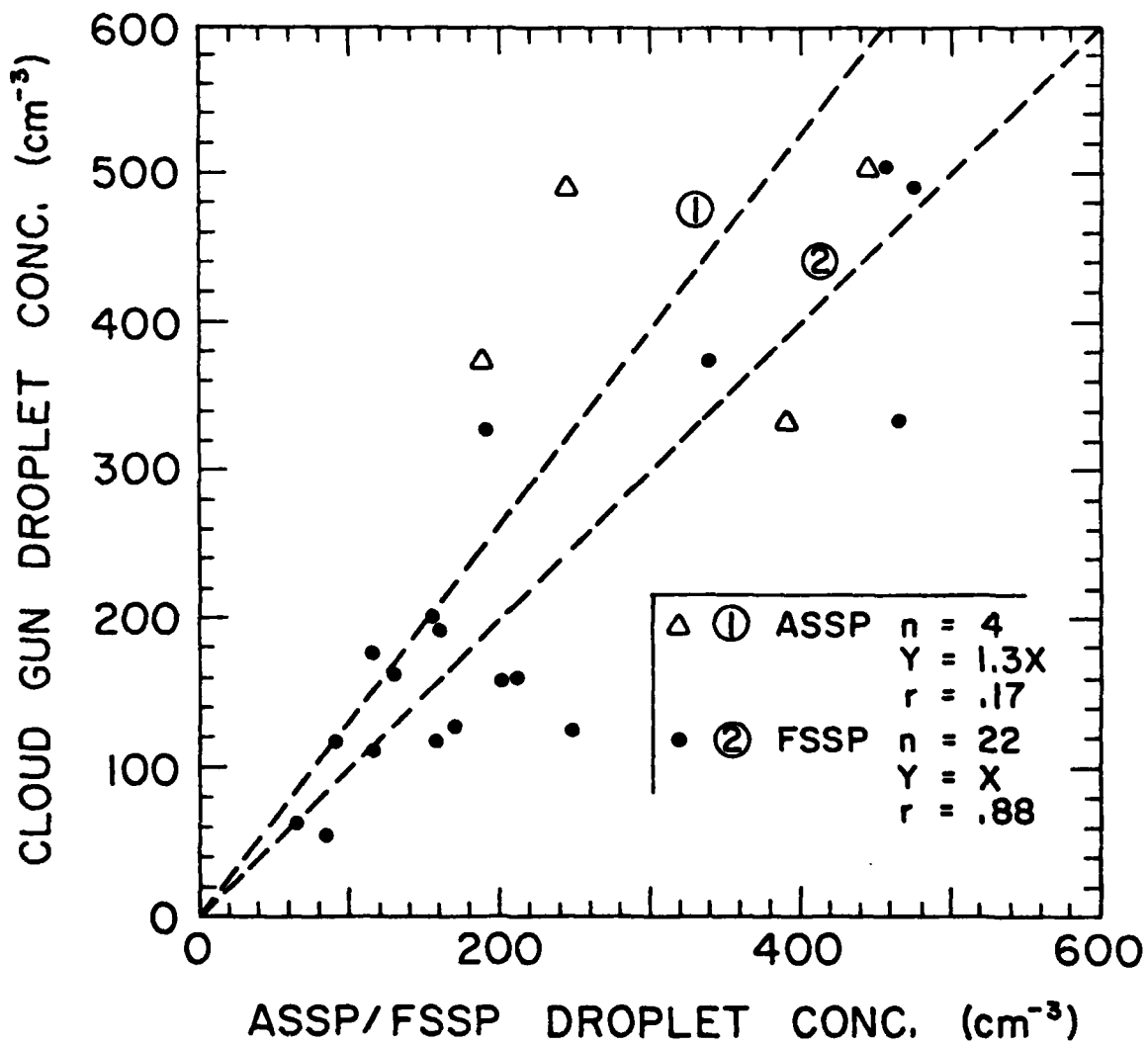


Fig. 16 Comparison of ASSP, FSSP and cloud gun-measured droplet concentrations for the 1980 field season.

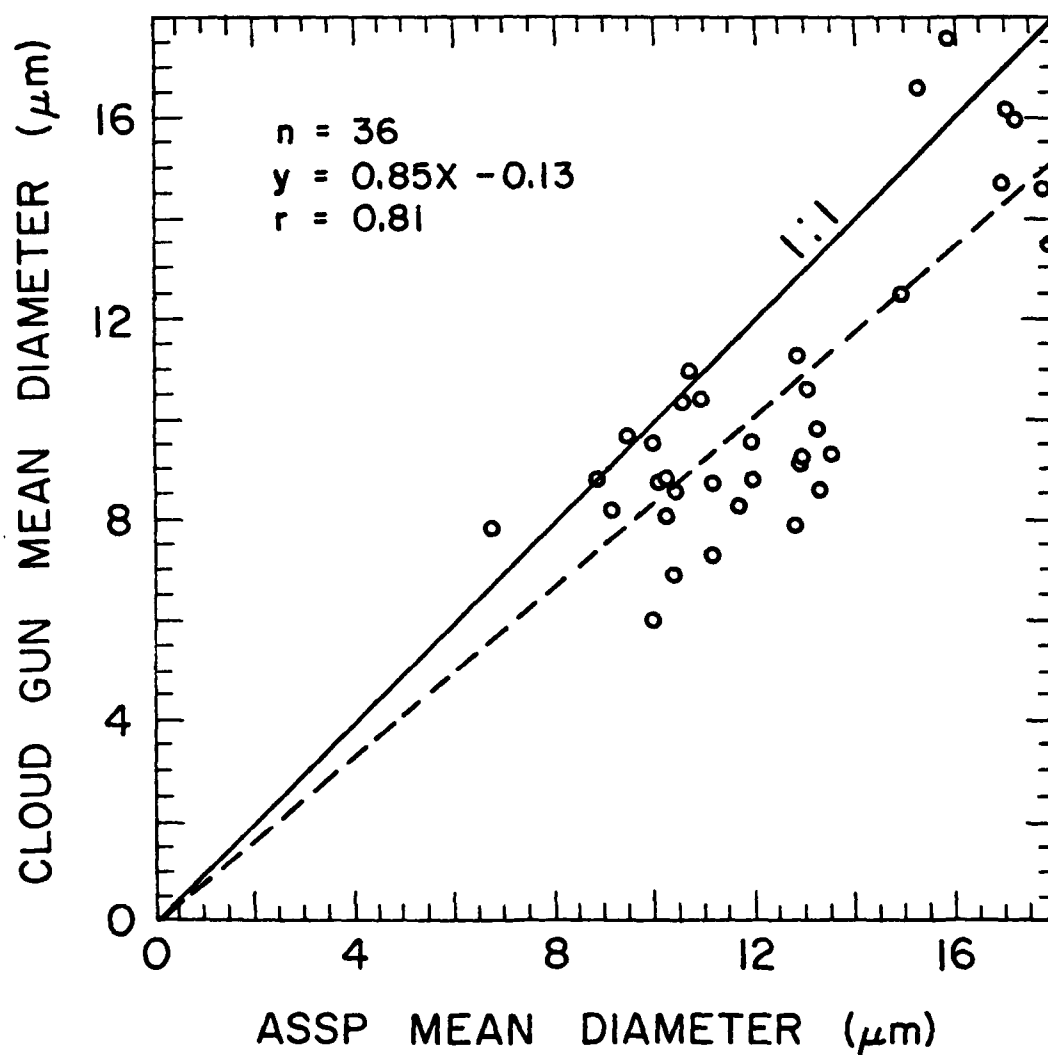


Fig. 17 Comparison of mean droplet diameters measured by the ASSP and cloud gun during the 1979 field season.

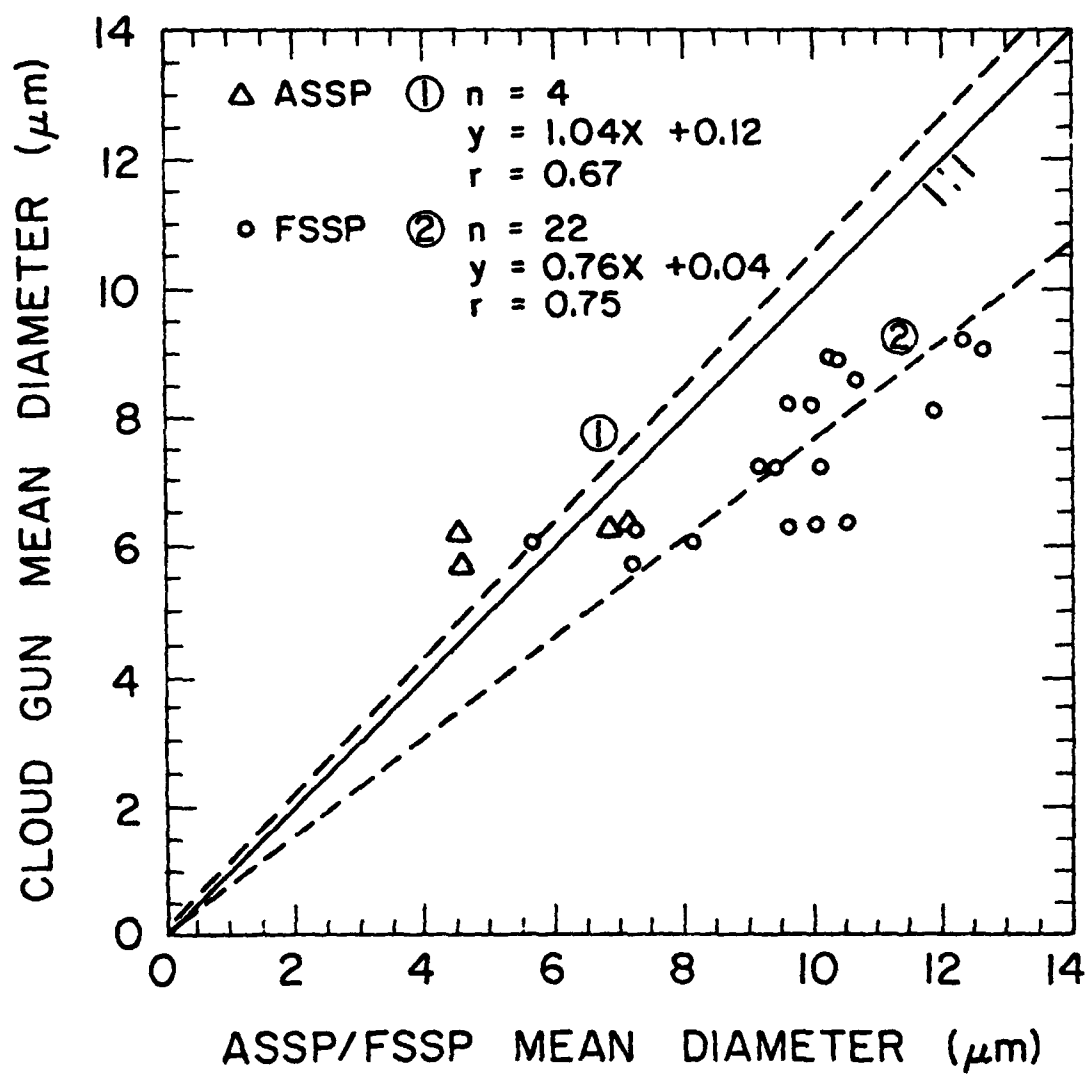


Fig. 18 Comparison of mean droplet diameters measured by the ASSP, FSSP, and cloud gun during the 1980 field season.

CG-measured values 15% lower than mean diameters as measured by the ASSP. The small amount of 1980 data show the two instruments in near agreement. So it can be concluded that better than 15% agreement could be expected in general, although the scatter for individual samples goes up to 30% and more.

The FSSP - CG comparisons show the CG-measured diameters to be on the average 76% of those measured by the FSSP. The correlation between the two instruments is good with a correlation coefficient,  $r = 0.75$ .

As a comparison of the measured widths of the droplet distributions, the standard deviations were computed and compared in Fig. 19. Both the ASSP and FSSP demonstrate similar spectral broadening and have standard deviations approximately twice those of the CG. The 1979 ASSP-CG comparisons shown in Fig. 20 indicated the same relationship.

For a period of 240 min, the ASSP, FSSP, and CSIRO probes sampled cloudy air simultaneously in the wind tunnel. A comparison of the droplet concentrations measured by the ASSP and FSSP is seen in Fig. 21. The FSSP appears to measure slightly higher concentrations than the ASSP as also indicated by Fig. 2. Although the ASSP and FSSP were installed side-by-side in the wind tunnel, it is interesting to note the amount of variability in the data as indicated by the correlation coefficient of 0.70.

The data in Fig. 21 and in subsequent comparisons of the ASSP, FSSP, and CSIRO probes were averaged over 2 s. Data from each instrument are recorded once each second; however, the ASSP's and FSSP's 1 s sample represents an average over that period, while the CSIRO probe's 1 s sample represents an instantaneous value. Data were used only when droplet concentrations were greater than  $100 \text{ cm}^{-3}$ , and when mean diameter measured by the ASSP was less than  $8 \text{ }\mu\text{m}$ . This latter restriction was based upon suspicious behavior of the ASSP when droplets were of larger size, due possibly to poor calibration in the larger channels. The cause for this behavior is still unknown; however, until a cause can be found, the data will only be compared for mean diameters less than  $8 \text{ }\mu\text{m}$ .

Fig. 22 shows a comparison of the mean droplet diameters measured by the ASSP and FSSP while mounted together in the wind tunnel. The variability

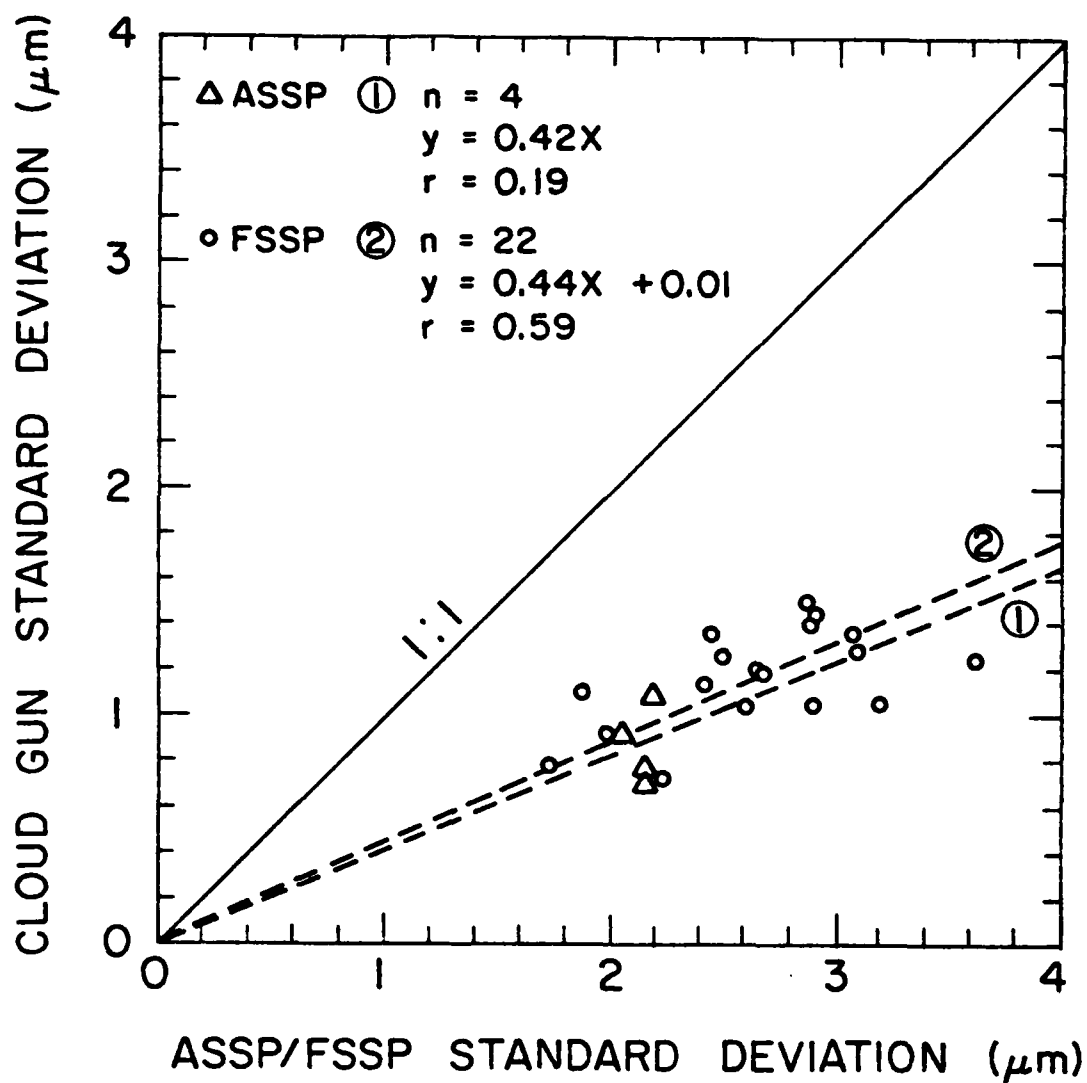


Fig. 19 Comparisons of the ASSP, FSSP and cloud gun-measured droplet spectra standard deviations during the 1980 field season.

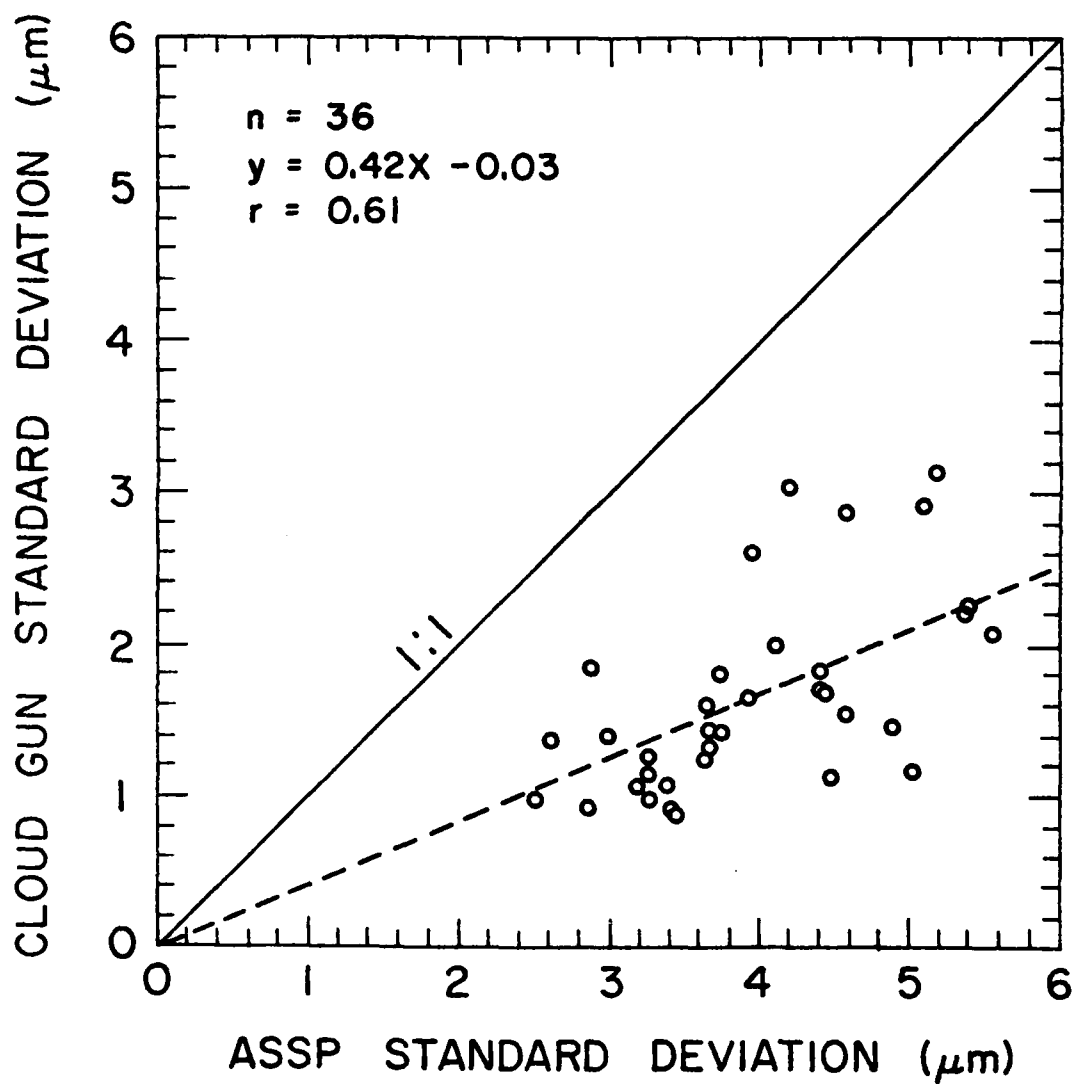


Fig. 20 Comparison of droplet spectra standard deviations measured by the ASSP and cloud gun during the 1979 field season.

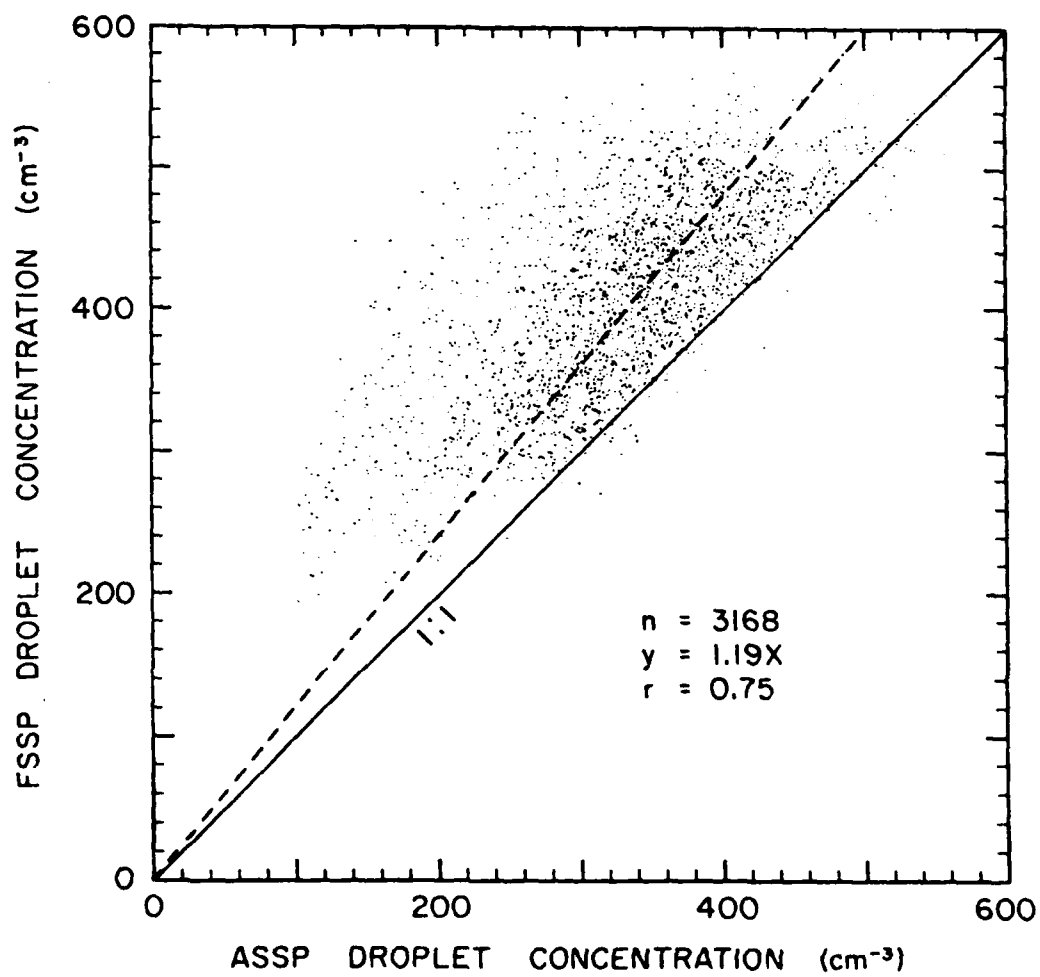


Fig. 21 Comparison of droplet concentrations measured by the ASSP and FSSP during a 240 min time period on 28 March 1980 at the Elk Mountain Observatory.

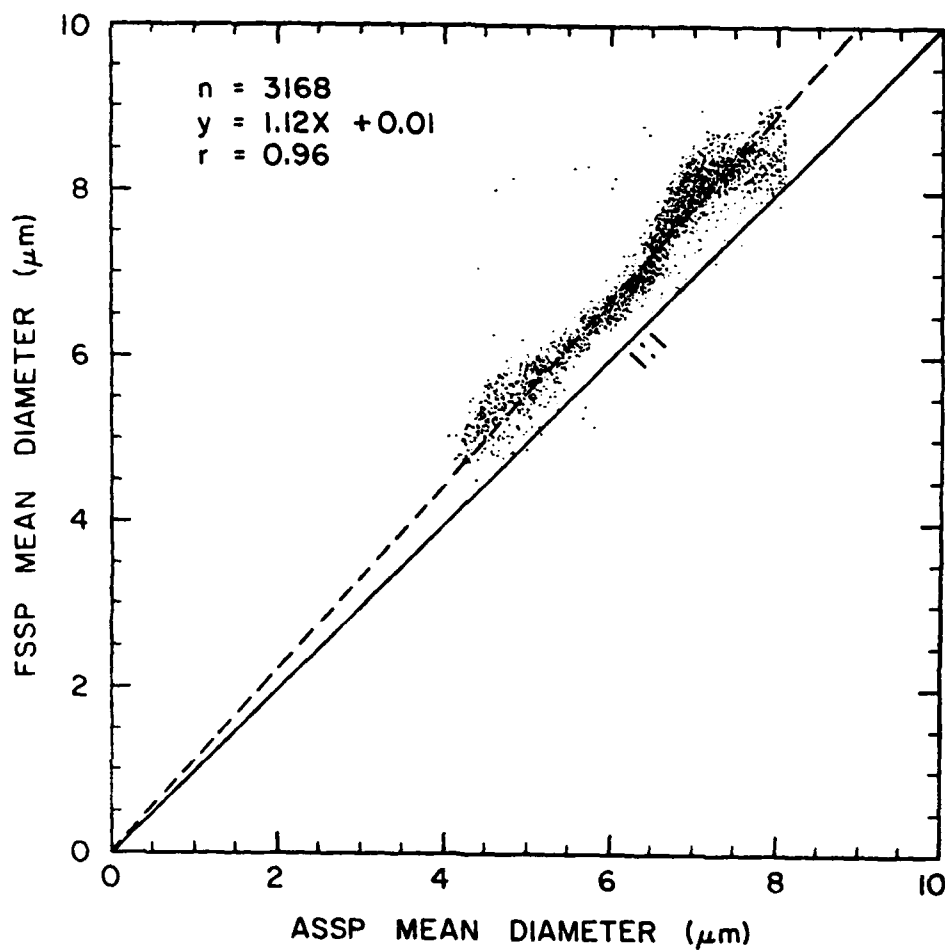


Fig. 22 Comparison of droplet mean diameters measured by the ASSP and FSSP. Sample is that described in Fig. 20.

of the data over this region is quite small: The correlation coefficient is 0.94. This comparison and the FSSP - CG comparison show that the FSSP indicates droplet distributions which are shifted slightly to larger sizes relative to the ASSP or CG measurements.

The widths of the size distributions indicated by the ASSP and FSSP are in reasonable agreement on the average as seen in Fig. 23. The ASSP appears to measure slightly wider spectra than the FSSP perhaps as a result of the ASSP's larger depth of field. These data show a large amount of scatter with a correlation coefficient of only 0.54.

Droplet size distributions are averaged over the entire 240 min period for each of the two droplet probes in Fig. 24. The two spectra are very similar, with that from the FSSP shifted by  $\sim 2.0 \mu\text{m}$  to larger diameters. Both instruments were operated in the 2 - 30  $\mu\text{m}$  size range so that this shift corresponds to one bin width.

## (2) Liquid Water Content Comparisons

The liquid water contents (LWC) measured by the CG are compared with those measured by the ASSP and FSSP in Fig. 25. The agreement between ASSP and CG - measured LWC's appears to be relatively good during the 1980 season and also during the 1979 season as shown in Fig. 26 which however is somewhat fortuitous in light of the discrepancies in indicated droplet concentrations. The underestimation of droplet concentrations are balanced by the overestimation of mean diameters and standard deviations in the calculation of LWC's. The FSSP measured larger LWC's than does the CG. It was shown that the FSSP and CG were in excellent agreement for concentration measurements and that the FSSP measures larger mean diameters than does the CG, thus, the major factor in these differences in LWC measurements lies in the spectral broadening introduced by the FSSP.

Fig. 27 shows a comparison between the CG and CSIRO probe. With only the 5 data points available little can be said beyond noting the large degree of scatter. In view of the difference in sampling times and sampled volumes considerable variability can be expected. Thus, the comparison can only serve as a rough indication of performance.

Fig. 28 shows a comparison between the ASSP and FSSP-measured LWC's. The variability is fairly small; the correlation coefficient has a value of 0.86. The FSSP measured LWC values  $\sim 1.2$  times greater than those

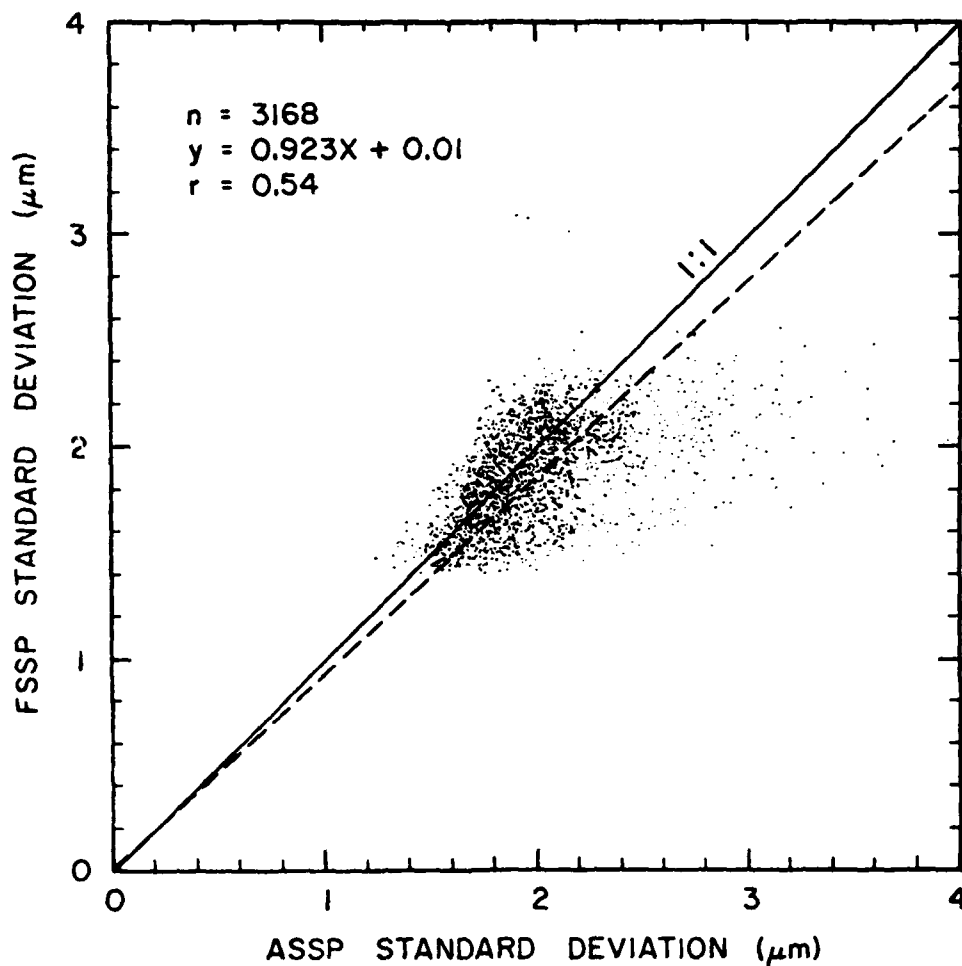


Fig. 23 Comparison of ASSP and FSSP-measured droplet spectra standard deviations. Sample is that described in Fig. 20.

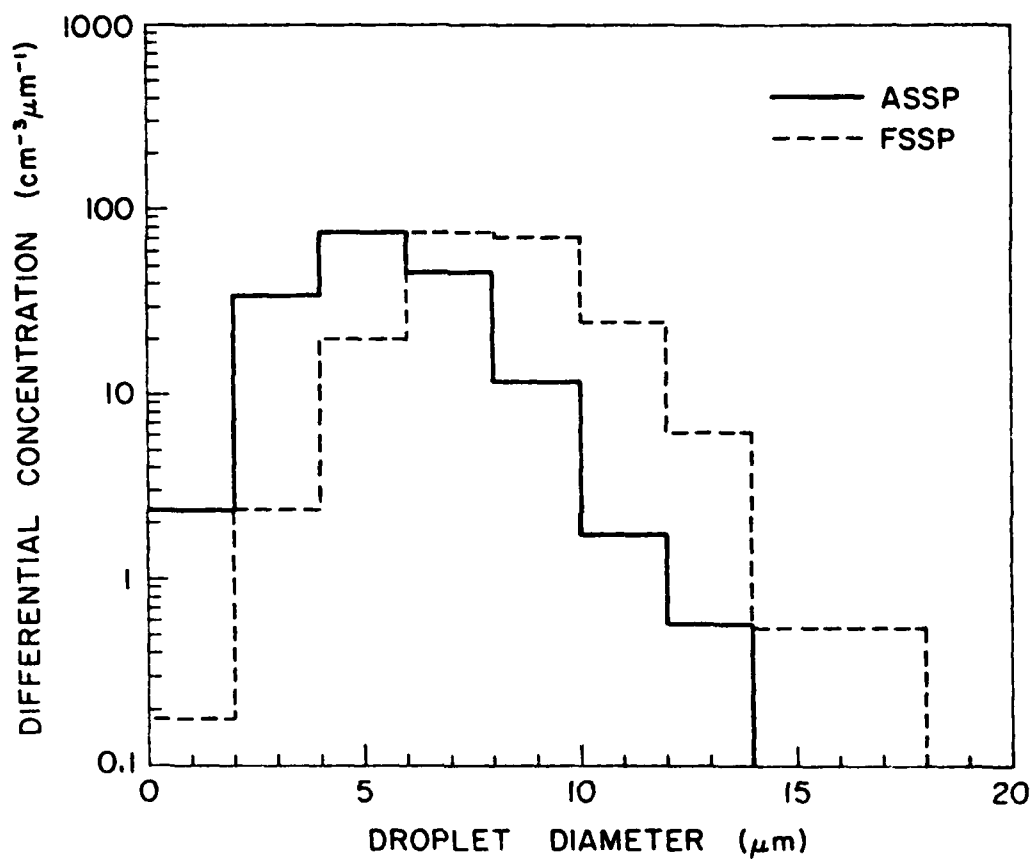


Fig. 24 Comparison of average droplet spectra measured by the ASSP and FSSP over a 240 min period on 28 March, 1980.

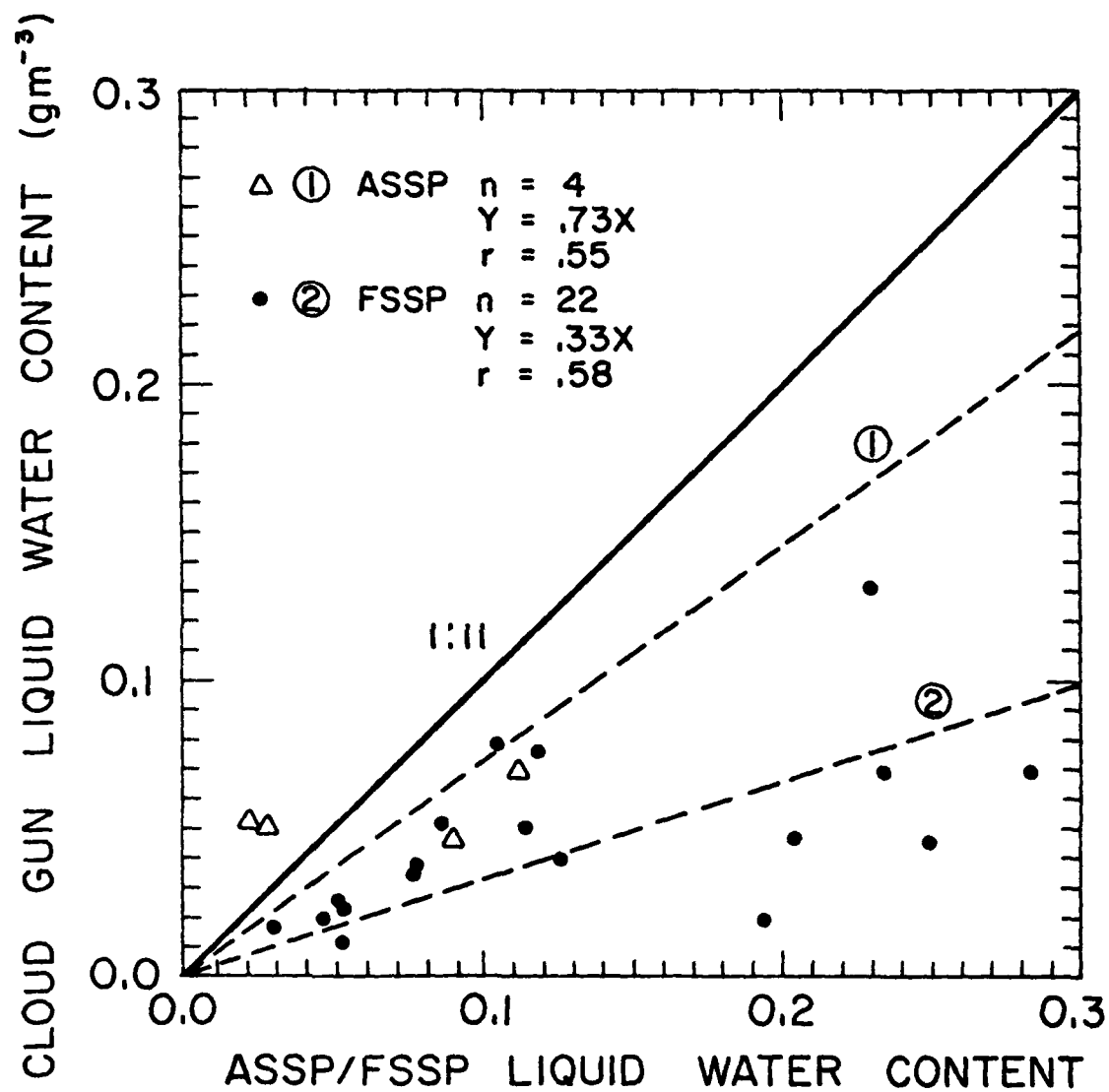


Fig. 25 Comparison of ASSP and FSSP-measured liquid water contents with those measured by the cloud gun during the 1980 field season.

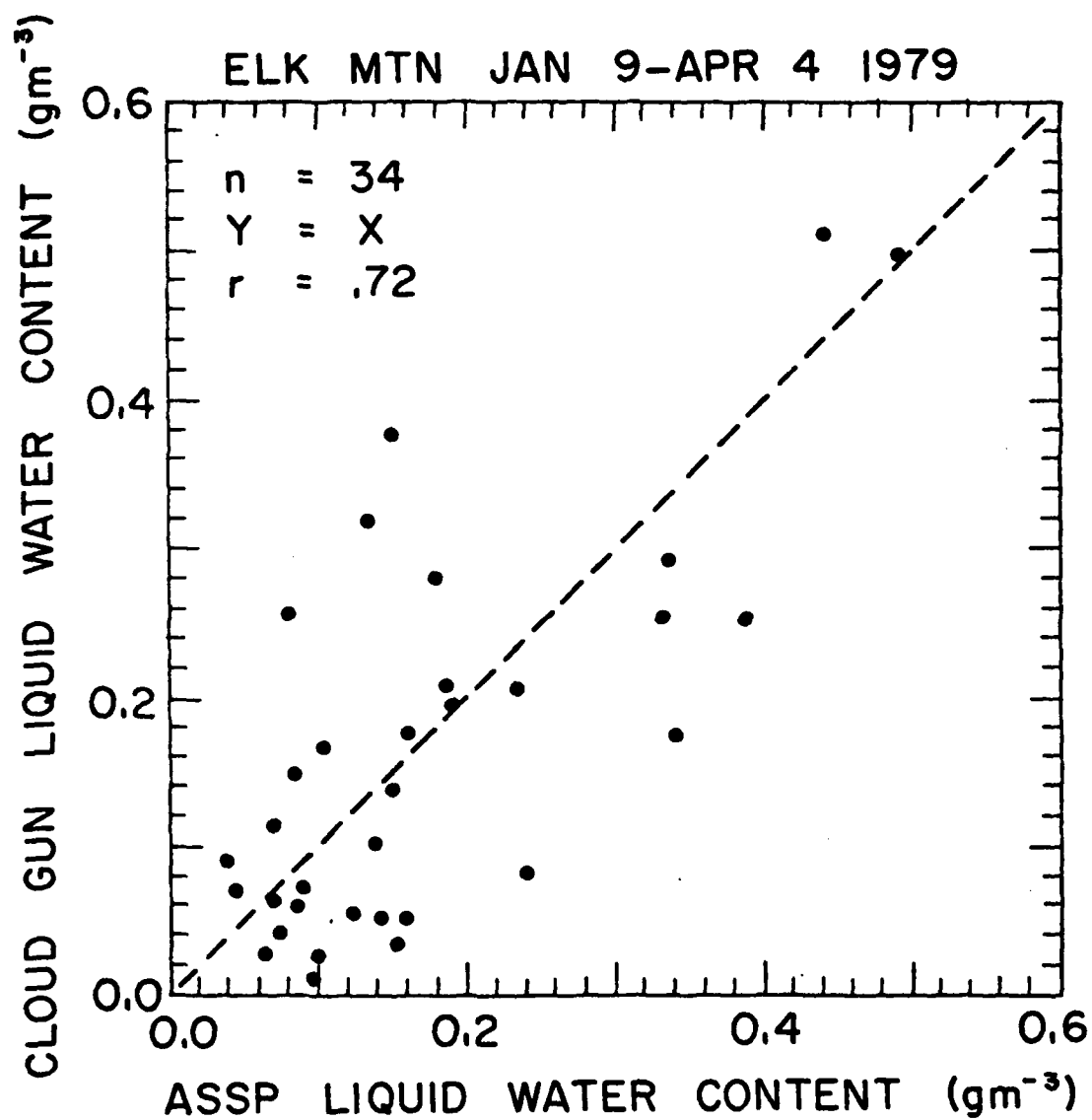


Fig. 26 Comparison of ASSP-measured liquid water contents with those measured by the cloud gun during the 1979 field season.

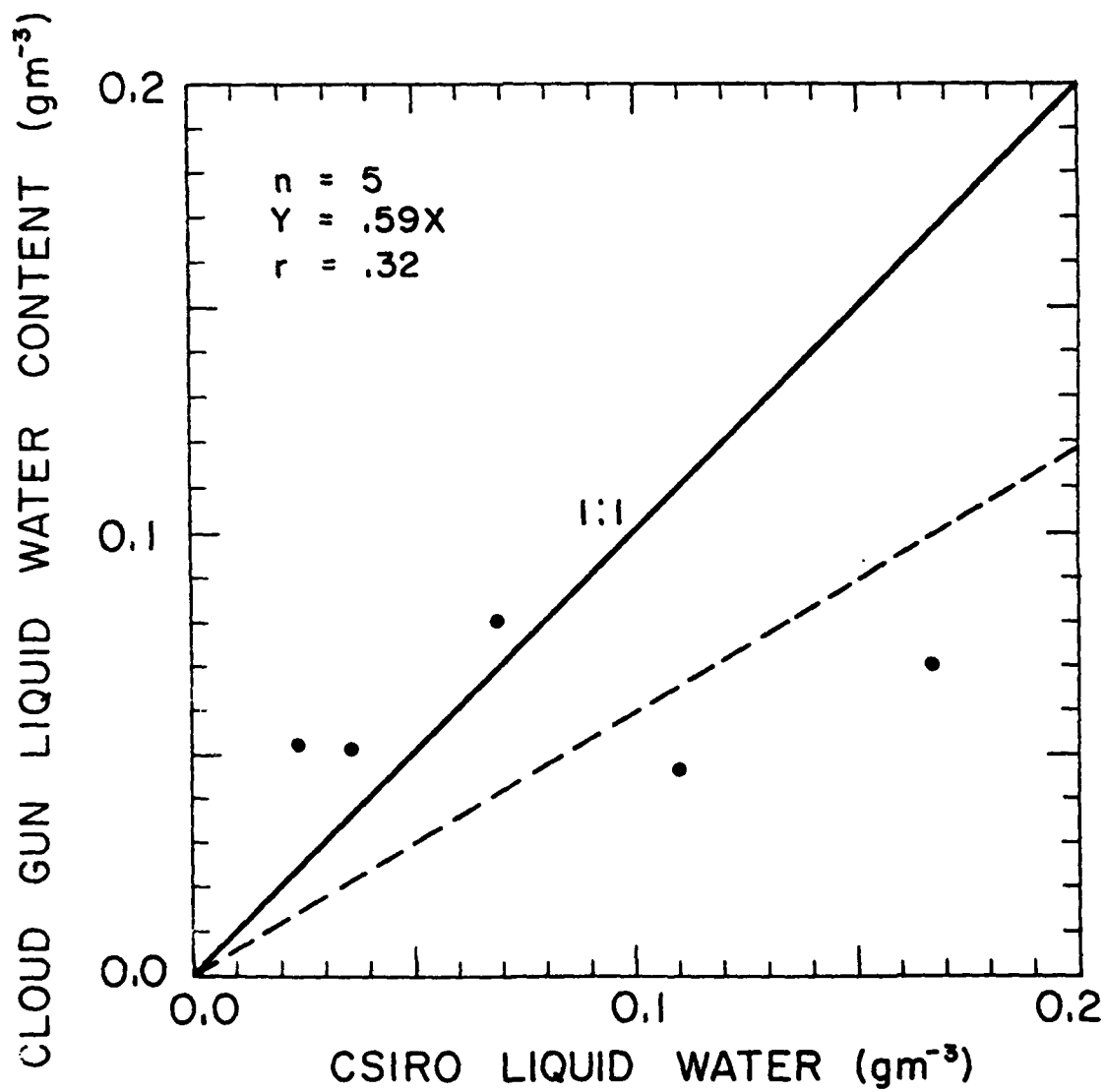


Fig. 27 Comparison of liquid water contents measured by the CSIRO probe and the cloud gun during the 1980 field season.

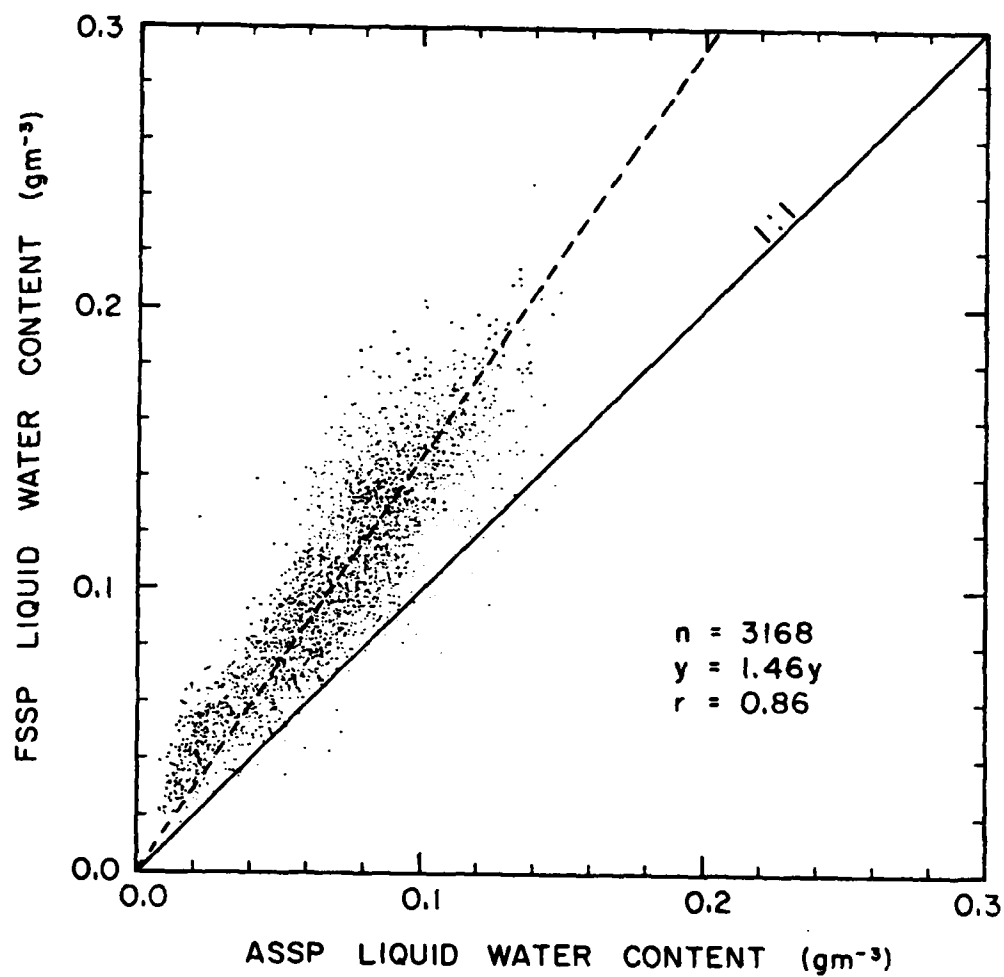


Fig. 28 Comparison of liquid water contents measured by the ASSP and FSSP during the 1980 field season.

measured by the ASSP which is not unexpected in light of the somewhat higher droplet diameters and concentrations measured by the FSSP.

The scattergram in Fig. 29 presents the comparison between the LWC values measured by the ASSP and CSIRO probes. Fig. 30 shows the comparison between the FSSP and CSIRO probes. The deviations from the 1:1 agreement evident in these graphs are not excessive and are in directions expected on the basis of concentration and size differences noted with respect to the CG. The lower correlation coefficient for the CSIRO-ASSP comparison is mainly a consequence of smaller range in LWC values indicated by the ASSP than the FSSP.

A five minute plot of LWC's measured by the ASSP, FSSP, and CSIRO is presented in Fig. 31 to show the similarity of instruments' response to fluctuations in LWC. The CSIRO values are somewhat larger than those from the ASSP and FSSP because the dry air power loss term was not subtracted from the values in this particular representation of the data. This term represents about  $0.15 \text{ g m}^{-3}$  of liquid water for the CSIRO probe.

### (3) Discussion of Evaluations; Error Sources

#### (a) The Cloud Gun

The number of droplets impacting upon the CG is a function of the relative speed of the airstream carrying the droplets, the amount of time which the slide is exposed to the airstream, and the collecting efficiency of the slide for droplets of different sizes. The collection efficiency of the slide is in turn dependent upon the shape and dimensions of the slide, the size of the droplets, and the velocity of the airstream.

The air velocity through the sampling aperture of the CG was measured with a pitot tube and a pressure gage with accuracies of  $\pm 1.0 \text{ ms}^{-1}$ , or  $\sim 5\%$  at the mean value of  $22 \text{ ms}^{-1}$ .

There is some uncertainty about collection efficiencies for collectors of ribbon geometry. Although the theoretical calculations of Ranz and Wong (1952) are generally used, the experimental results of May and Clifford (1967) and Starr (1967) cast some doubt upon the validity of the theoretical values. Comparison of theoretical and experimental values show the latter to be 10% lower for  $10 \mu\text{m}$  diameter particles, and 23% lower at diameters of  $5 \mu\text{m}$ .

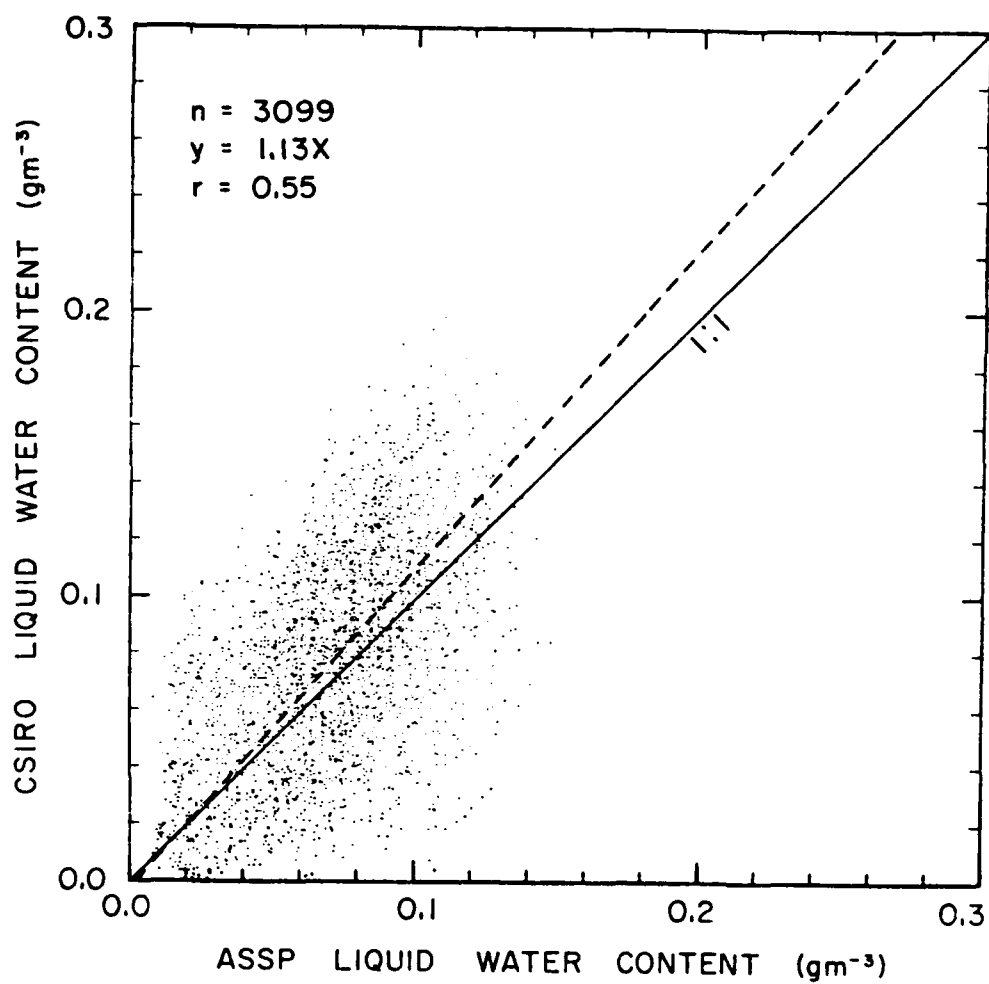


Fig. 29 Comparison of liquid water contents measured by the ASSP and CSIRO probe during the 1980 field season.

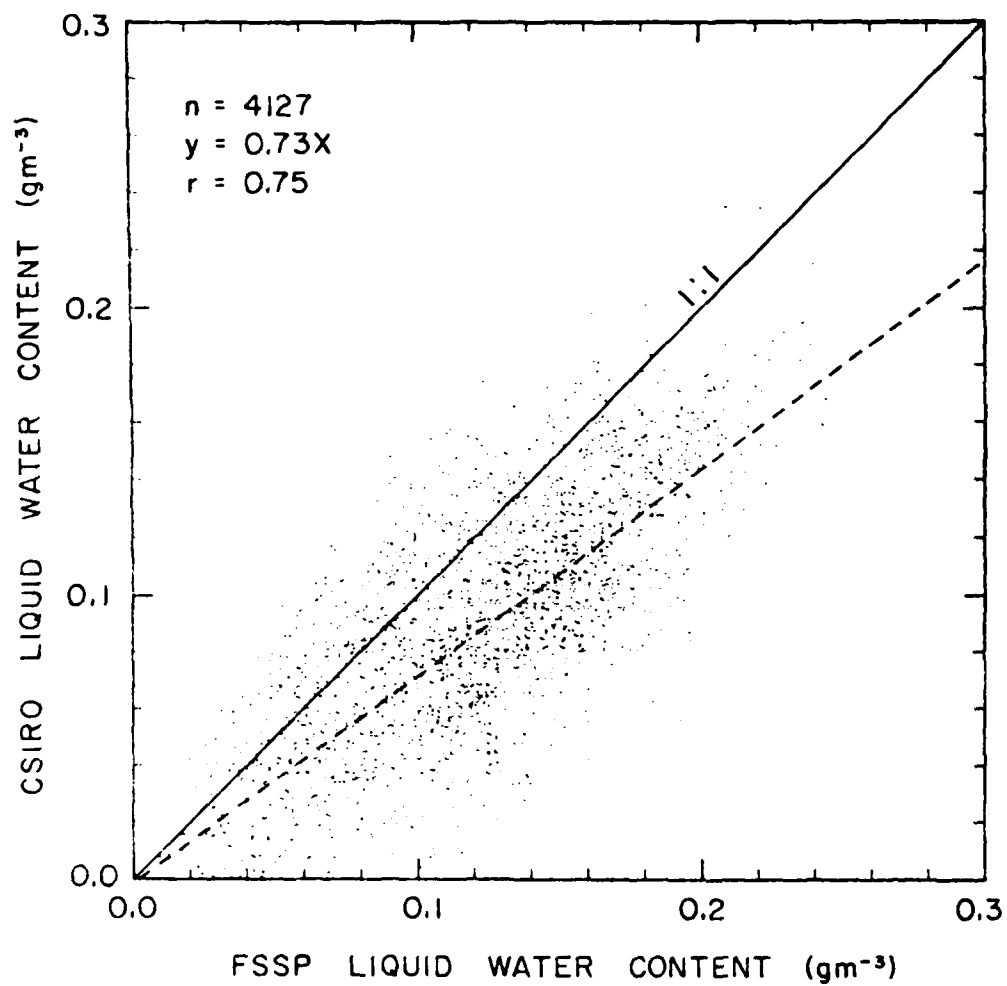


Fig. 30 Comparison of liquid water contents measured by the FSSP and CSIRO probe during the 1980 field season.

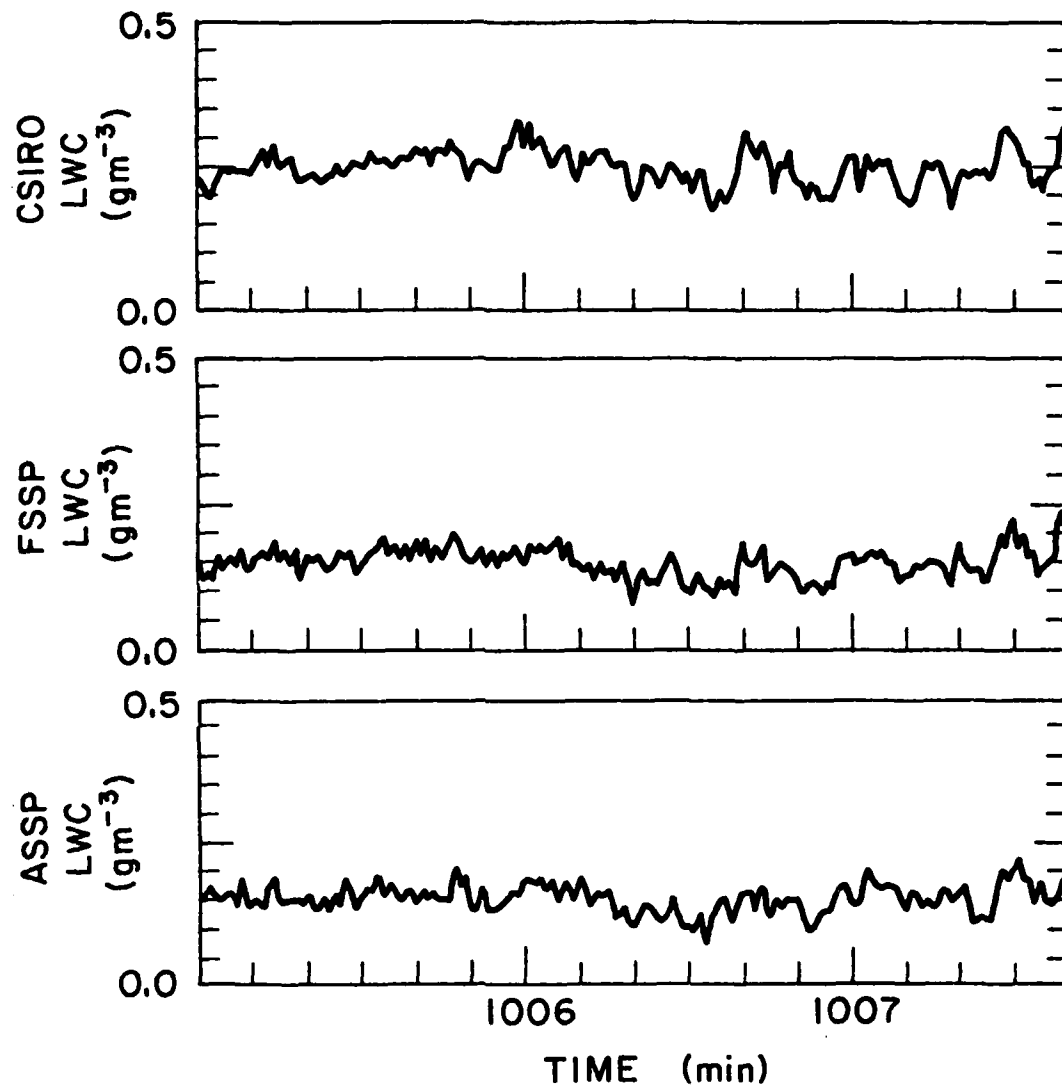


Fig. 31 The response of the CSIRO, FSSP and ASSP to fluctuations in liquid water content are compared for a sixteen minute portion of data taken during the 1980 field season.

Errors also arise in the analysis of the slides after they are exposed. The largest factor of uncertainty occurs in the derivation of the droplet size from the crater size. Squires and Gillespie (1952) performed calibrations relating droplet and crater diameters. Squires estimates that his calibrations are accurate to 5% for droplet diameters greater than 20  $\mu\text{m}$  and 15% for droplets less than this size. Most of the droplet spectra seen during the Elk Mountain project have mean diameters less than 20  $\mu\text{m}$ . Thus, droplet concentrations from cloud gun data are expected to be accurate to perhaps 20%; droplet diameters to about the same value, and derived LWC values to  $120\% \times (120\%)^3$ : about a factor of two in the worst case.

(b) The ASSP and FSSP

Errors in the response of these instruments are functions of the optical properties and the electronic response characteristics.

Droplet distributions are artificially broadened due to the lack of uniformity of laser light intensity across the beam diameter and because droplets have also been found to be sized differently across the defined depths of field of these instruments.

Other sources of systematic oversizing arise from background scattering of droplets passing outside the depth of field and also from multiple scattering due to coincident droplets at higher droplet concentrations. These sources of error are expected to contribute little to the Elk Mountain data because droplet concentrations rarely exceeded  $500 \text{ cm}^{-3}$  during our sampling.

Errors in the determination of droplet concentrations arise due to deadtime errors and variable sampling volumes. Because the instruments require a finite amount of time to process pulses produced by droplets passing through the beam, the electronics will be unable to detect any other particles passing through the beam during that time. The FSSP is less susceptible to such errors due to design improvements. The ASSP is delayed the same amount of time whether the droplet passes within the depth of field or not. Also this particular version of the ASSP is delayed an additional period if a droplet enters the sample volume while it is busy processing the previous droplet. On the other hand, the FSSP does

not have this latter liability, and any droplet passing outside the depth of field will only cause a delay a fraction of the normal processing delay.

The effective sampling volume of the ASSP and FSSP depend upon the fraction of the beam diameter from which pulses are electronically accepted. This fraction is determined by averaging the transit time of particles passing through the beam. Any particles having transit times less than the average are rejected. The averaging time can be effected by droplet speed, diameter, and concentration. Uncertainty in the determination of the effective sample volume can thus be the largest source of error when determining droplet concentrations from these two instruments.

(c) The CSIRO Liquid Water Probe

The major source of error in LWC using the CSIRO probe arises from uncertainties in collection efficiencies. Experimental data show that the probe should have an 85 to 95% efficiency in collecting droplets with diameters of 10  $\mu\text{m}$ . The data in this report have not been corrected for this error. Another source of uncertainty in the measurements lies in the "dry air calibration", that is, the background response to changes in airspeed and temperature.

e. Study of the Response of the ASSP to Ice Particles

Some of the studies conducted on the response of the ASSP and FSSP to ice particles were reported briefly in Scientific Report No. 1.

Under conditions when no (or few) water droplets but numerous particles are present, the ASSP and FSSP respond with counts in a flat distribution across the entire spectrum. If water droplets are present, the droplet spectrum is superimposed upon this flat distribution (see Fig. 32). In Scientific Report No. 1 we noted that the flat "tails" of the ASSP and FSSP distributions appeared to change in proportion with the ice particle concentration, but indicate concentrations 2 1/2-3 orders of magnitude higher than the actual ice particle concentration.

We compared concentrations of particles within the tails of the droplet distribution with ice particle concentrations measured by the 1D-C or 2D-C probe. The ASSP spectrum was truncated to include only the flat part, which we assume is due to ice particles above a certain although somewhat arbitrary, size for comparison. These spectra were

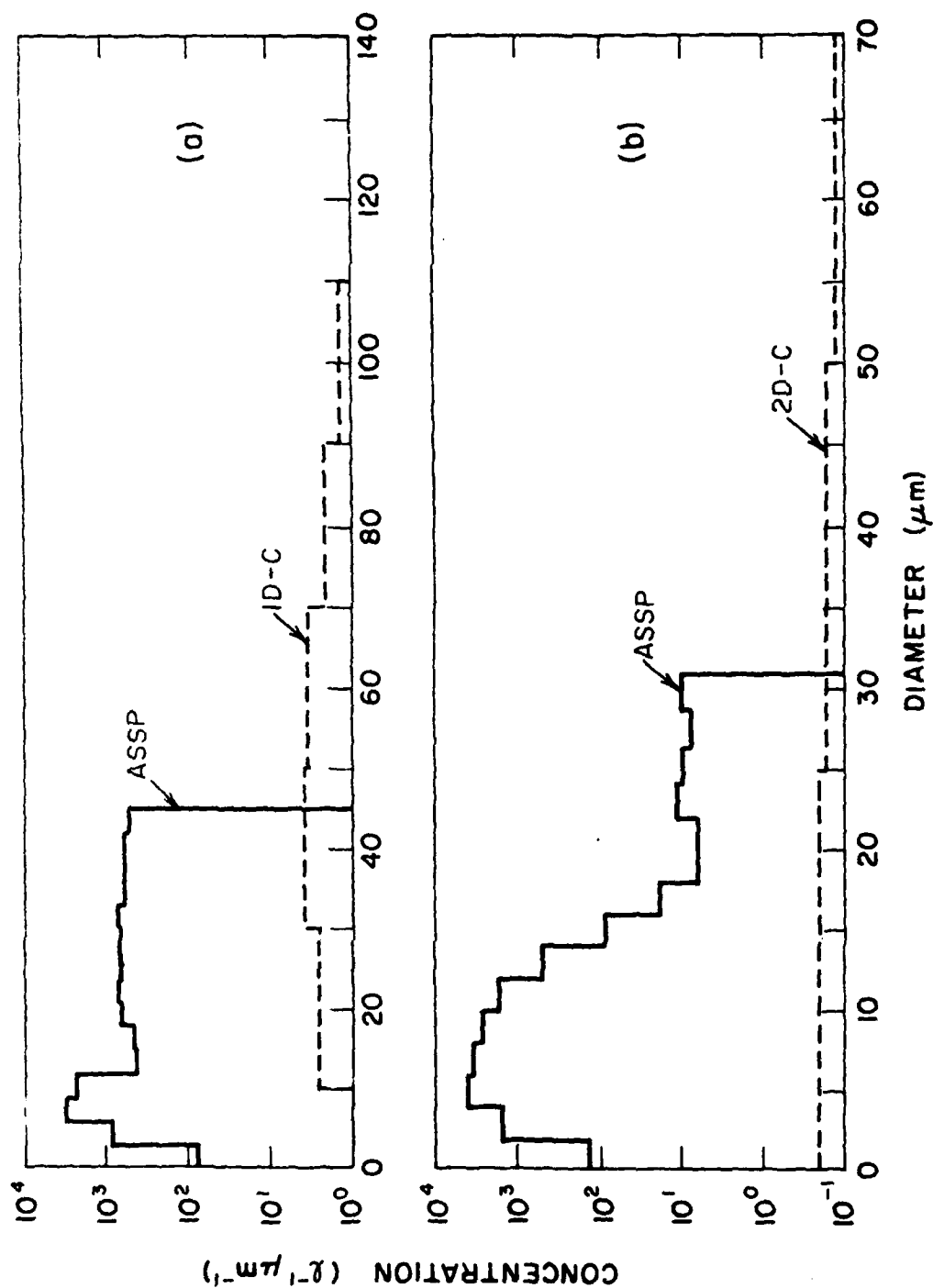


Fig. 32 Cloud particle size distributions measured by the ASSP and 1D-C or 2D-C probes at the Elk Mountain Observatory. (a) 4 April 1979, 111130-111200 MST, ASSP  $N=37 \text{ cm}^{-3}$ , ASSP "ice"  $\sim 19,000 \text{ l}^{-1}$ , 1D-C  $N = 282 \text{ l}^{-1}$ . (b) 19 March 1980, 203530-203600 MST, ASSP  $N = 28 \text{ cm}^{-3}$ , ASSP "ice"  $\sim 150 \text{ l}^{-1}$ , 2D-C  $N = 61.2 \text{ l}^{-1}$ .

truncated by inspection. These false ice concentrations were plotted against corresponding 1D-C or 2D-C ice crystal concentrations in Fig. 33. The data points represent 30 s averages from both data sources.

The conclusion which can be drawn from Fig. 33 is that ASSP or FSSP data are definitely erroneous if these ice concentrations are present in excess of  $10 \text{ L}^{-1}$ . The shape of the ASSP or FSSP spectrum allows such faulty data to be recognized relatively easily, and a rough correction can be made. Note that the response of the droplet probes to ice particles is a small fraction of the droplet concentration in a mixed cloud and in most cases no corrections are necessary. It can be anticipated that different crystal habits produce different ASSP and FSSP responses; for example, large crystal aggregates might produce even higher false counts. This factor may limit the general validity of the data shown in Fig. 33.

#### 5. Summary and Conclusions

From the studies conducted and discussed in this report we have derived the following conclusions concerning measurements of cloud particle spectra:

The 1D-C probe undercounts particles in the lower channels ( $\sim 140 \text{ }\mu\text{m}$ ) due to decreased depths of field for these small sizes. The problem is two-fold: the probe tends both to undercount and missize particles. An iterative correction scheme to account for both effects is needed to correct the indicated spectra but is prohibitively cumbersome for realtime use. PMS' corrections and those which we derived in 1979, based on 11 comparisons with O-H data, appear to do a reasonable job for channel-by-channel corrections. The agreement in data from the 1979 and 1980 bead tests suggest to us that our results can be successfully applied to other PMS 1D-C probes.

The 2D-C probe undercounts and missizes particles in the smaller channels due to reduced depths of field in these sizes. We have used both PMS' corrections and our own iterative technique to correct this with little success and recommend use of a constant depth of field (no small channel correction for 2D-C data analysis. We have no reason to suspect that these results are not applicable to other 2D-C probes.

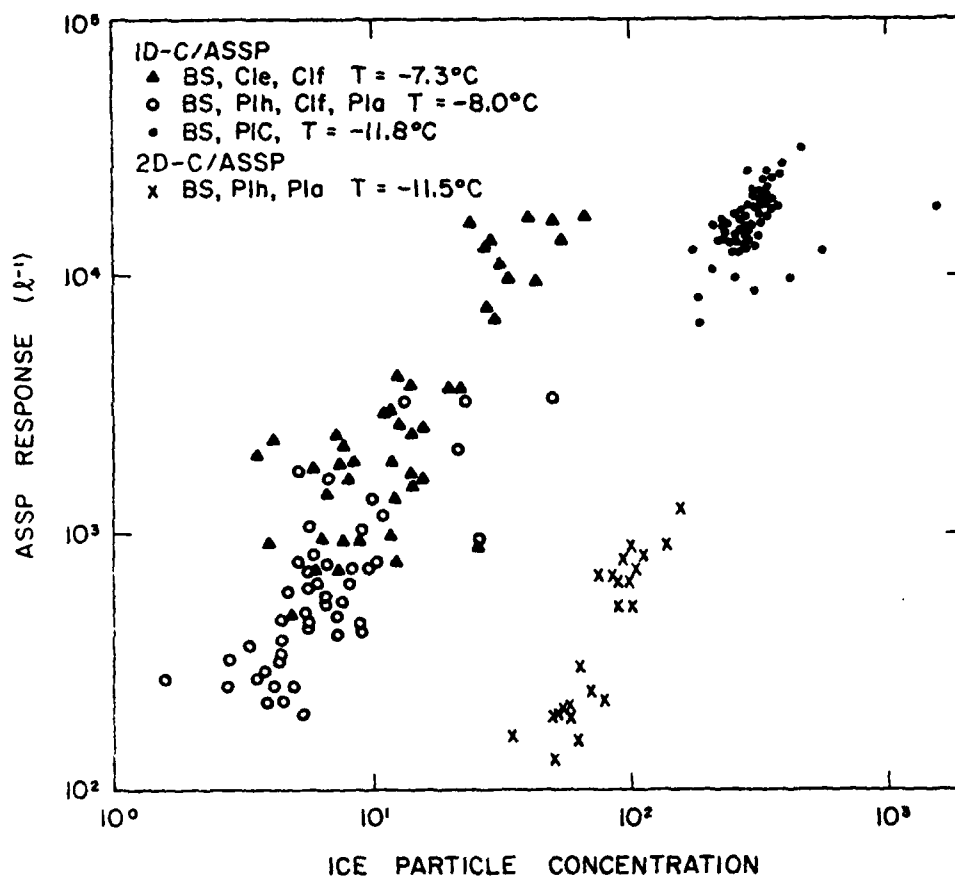


Fig. 33 The ASSP response to ice particles plotted against the ice particle concentrations measured from the 1D-C or 2D-C probes. The method used to determine the ASSP response is described in the test. All data are from the Elk Mountain Observatory on (▲) 16 March 1979, (○) 17 March 1979, (•) 4 April 1979 and (x) 19 March 1980.

Work is underway at our Department to reconstruct a true ice spectrum from the spectrum measured in a mixed-phased cloud, using the depolarization data.

Errors which affect the response of the cloud gun (CG), ASSP, FSSP and CSIRO when measuring cloud droplet spectra have been analyzed. The accuracy of measurements by the CG is primarily affected by uncertainties in droplet collection efficiencies of the soot-coated slide and droplet-to-crater size calibrations at diameters smaller than 20  $\mu\text{m}$ . The ASSP and FSSP artificially broaden droplet spectra due to nonuniformities in beam intensity. Errors in droplet concentration measurements arise because of uncertainties in sample volume determination and droplet counting losses during instrument deadtimes. The CSIRO probe is also subject to error in collection efficiencies, especially with droplets of less than 10  $\mu\text{m}$ . The need for accurate dry air power loss calibration is evident.

A comparison of droplet spectra and liquid water contents measured by the instruments was made while they were mounted in the Elk Mountain wind tunnel. The agreement between droplet concentrations measured by the CG and FSSP was excellent; however, the ASSP appears to measure smaller concentrations than either the CG or FSSP due to greater deadtime losses.

Comparison of droplet mean diameters measured by the CG, ASSP, and FSSP indicate a one-to-one agreement between the ASSP and CG with the FSSP measuring slightly higher diameters than the other two instruments. Both the ASSP and FSSP have more than twice the measured standard deviations of the CG.

Primarily because of the artificial broadening of the droplet spectrum by the ASSP and FSSP, these instruments measure liquid water contents typically two to three times higher than the CG. Comparisons with the ASSP and FSSP indicate that the FSSP measures liquid water contents which are 50% higher than the ASSP due to the larger mean diameters and concentrations measured by the FSSP. The CSIRO and ASSP agree well in their measured liquid water content values although the measurements show a fair amount of scatter. The FSSP measures liquid water contents approximately 25% higher than the CSIRO.

It needs to be emphasized that the results given in this report are in some respects specific to the particular instruments used in the tests. The extent of this specificity is difficult to assess, to that great care should be taken in adapting these results to data from other, even apparently identical instruments. Other units may be either better or worse; the units used in these tests were not of unusual design or with many special features; on the other hand, great care was taken with their calibrations, and each instrument's history was well-documented.

## REFERENCES

- Baumgardner, D.G., 1980: A critical analysis and comparison of four water droplet measuring instruments. M.S. Thesis, Department of Atmospheric Science, College of Engineering, University of Wyoming, 167 pp.
- Baumgardner, D.G. and G. Vali, 1980: Empirical evaluation of airborne liquid water devices. Papers presented at the Third WMO Scientific Conference on Weather Modification, Clermont-Ferrand, FR, 21-25 July 1980.
- King, W.D., D.A. Parkin and R.J. Handsworth, 1978: A hot-wire liquid water device having fully calculable response characteristics. J. Appl. Meteor., 17, pp. 1809-1813.
- May, K.R., and R. Clifford, 1967: The impaction of aerosol particles on cylinders, spheres, ribbons and disks. Ann. Occupational Hygiene, 10, p. 83-95.
- Ranz, W.E. and J.B. Wong, 1952: Impaction of dust and smoke particles. Industrial and Engineering Chemistry, 44, p. 1371-1381.
- Squires, P. and C.A. Gillespie, 1952: A cloud droplet sampler for use on aircraft. Quarterly Journal of the Royal Meteorological Society, 78, p. 387-393.
- Starr, J.R., 1967: Inertial impaction of particulates upon bodies of simple geometry. Ann. Occupational Hygiene, 10, p. 349-36.
- Vali, G., M. Politovich, D. Baumgardner and W.A. Cooper, 1980: Conduct of cloud spectra measurements. Scientific Report No. 1 to the Air Force Geophysics Laboratory, Contract no AFGL-TR-79-0251.

## APPENDIX A

## Ice Particle Collection and Photography

The reference standard used to determine "true" ice crystal concentrations and size distributions is impaction and collection on mineral oil-coated glass microscope slides. These slides are exposed in the wind tunnel or from the observation platform for periods of 2-10 s, depending on ice crystal concentration. They are then brought into the cold room at the Observatory and immersed in a bath of cold hexane for photography. Aircraft O-H samples are exposed in a decelerator which reduces the impaction velocity by a factor of eleven. They are stored in chilled Dow 330 silicone compound until immersed in hexane for photography in the same manner as ground-based samples.

We use this method as our standard but do not claim it to be infallible. Often, too many crystals are collected on a slide which makes them difficult to count and size correctly. Collection efficiencies for sizes  $\leq 100 \mu\text{m}$  are uncertain. Above that size they are very close to unity. For determination of correction factors a collection efficiency of 80% was used for crystals in the smallest (to 20 or 25  $\mu\text{m}$ ) size bin, and 100% efficiency was assumed otherwise. We have observed crystals with diameters near 10  $\mu\text{m}$  on many slides, but it is not certain how well they represent true concentrations at that size. Nevertheless, the directness and simplicity of this sampling method is our basis for using it as a reference.

Several examples of particles collected on O-H slides are shown in Figs. A1-3. Minute structural details of ice crystals can be examined using this method. An observer can also use a probe to move crystals around on the cold slide in order to examine them more closely.

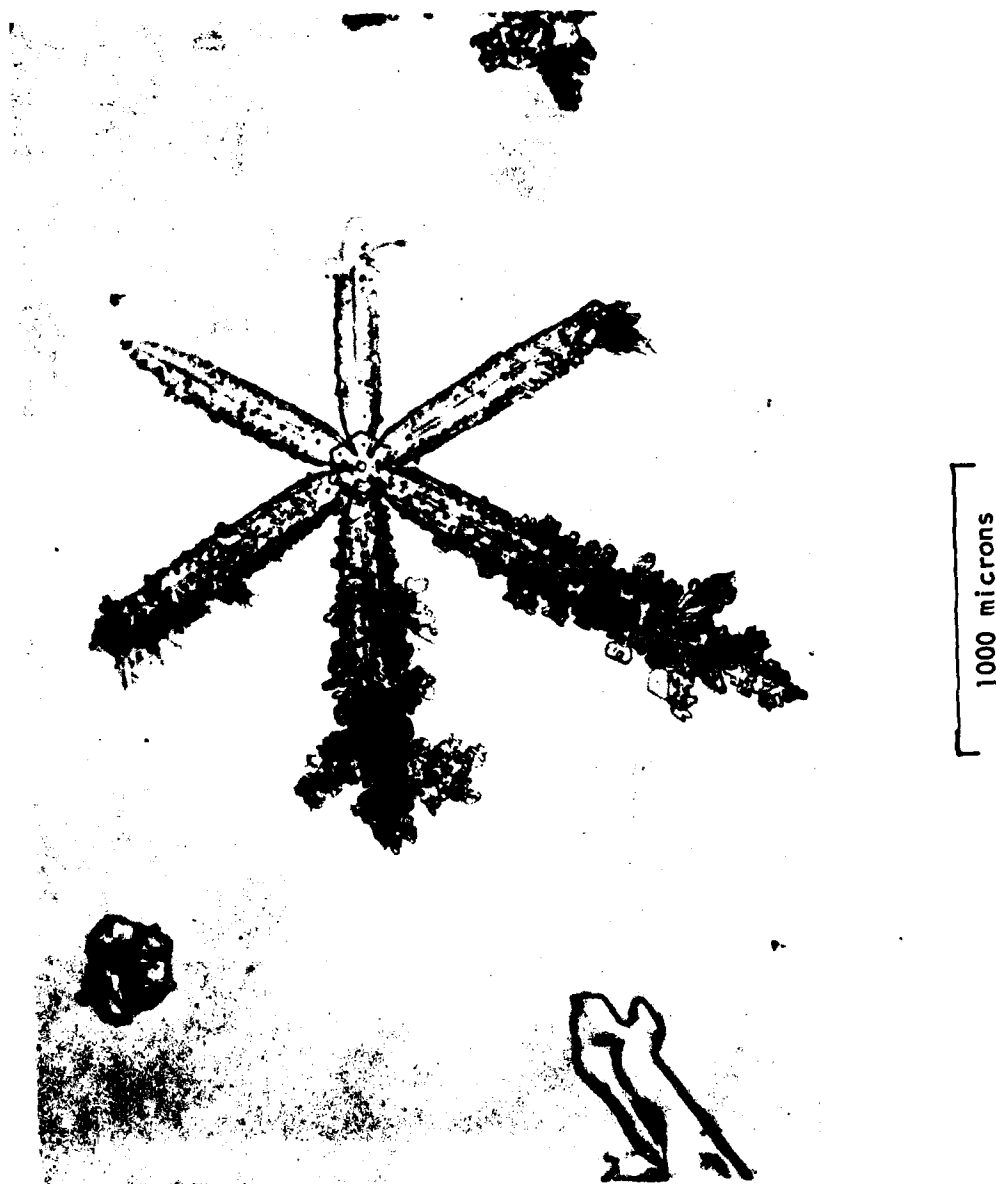


Fig. A1 Stellar crystal (pic-r) with light-moderate rime plus blowing snow particles.



Fig. A2 Grains of blowing snow.

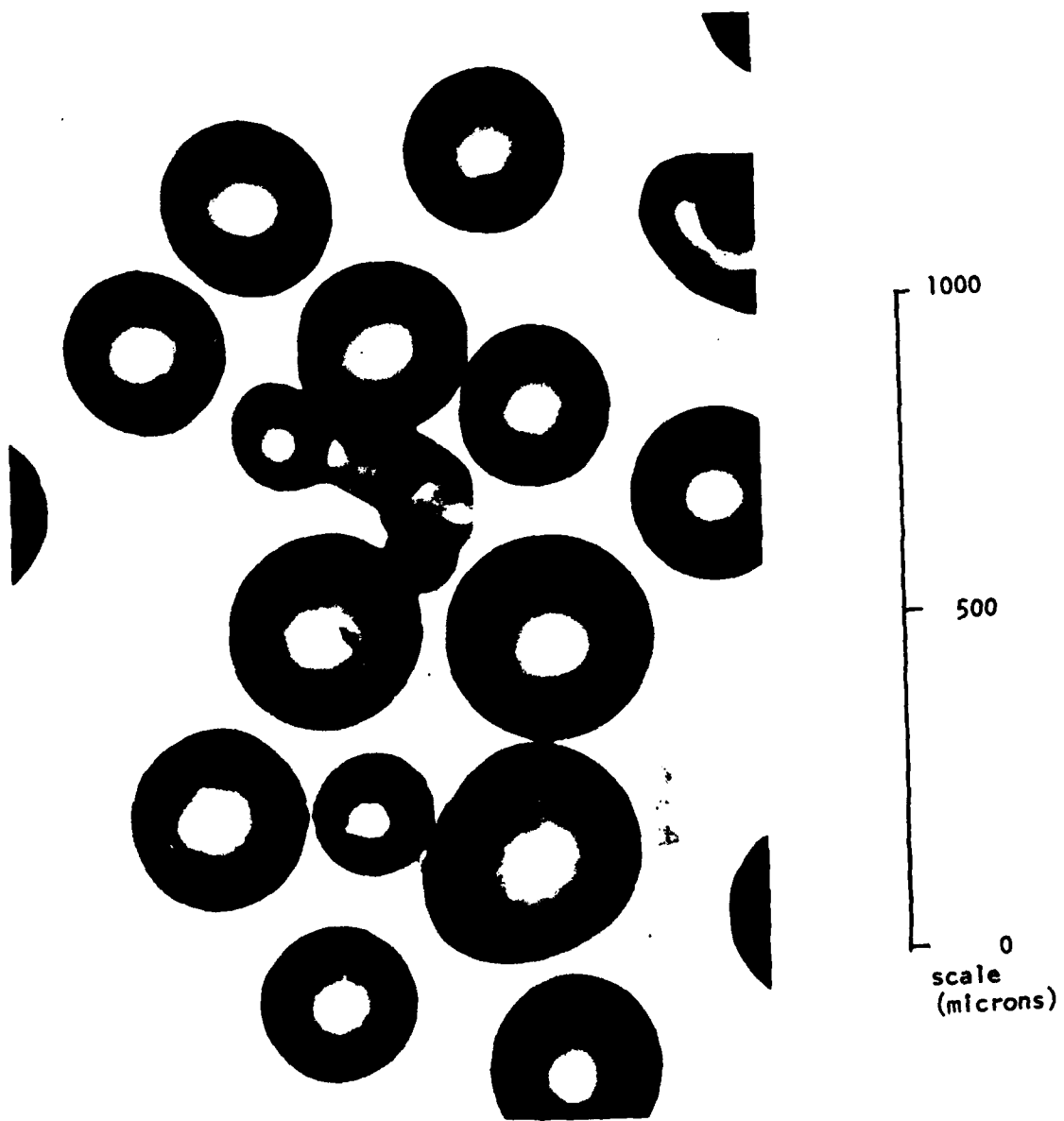


Fig. A3 Samli glass beads 250-300  $\mu\text{m}$  diameter.

## APPENDIX B

## THE CLOUD GUN

The "cloud gun" is a cloud droplet sampling device which has been used at the University of Wyoming for a number of years. It is based upon the design of Squires and Gillespie (1952). A CO<sub>2</sub> pistol propels a soot-coated glass slide, ~0.8 cm<sup>2</sup>, past a sampling aperture. Droplets impact upon the slide and leave a crater in the soot which is related to the droplet size. Timing of the slide exposure is accomplished by means of a photo electric circuit, and is recorded on magnetic tape with the other data collected at the Observatory.

Once the slide is exposed and its exposure time recorded by the data system it is returned to the laboratory and photographed under a microscope. Typically, the slide is photographed at random positions such that a fair representation of the entire slide surface is recorded. The film negatives are later enlarged and sized using a Zeiss TGZ3 particle sizer. Typically, 300-600 craters are counted to produce a size spectrum from a single slide.

Fig. B1 shows droplet craters from a soot-coated slide.

Although we have used this method of droplet sampling as a standard, uncertainties remain in analysis of data using the cloud gun. As can be seen in Fig. B1, the actual crater size can be difficult to determine. Accurate determination of airspeed, crater-to-droplet diameter ratios and time of the slide (determined to 10ths of a millisecond only) are a few of the difficulties encountered by using this system. Baumgardner (1980) has addressed these and other problems in detail and has determined that these uncertainties are small ( $\pm 10\%$  in concentration and  $\pm 15\%$  in droplet size).

The CG technique can measure droplet sizes from  $<1$  to  $>60$   $\mu\text{m}$  and can resolve fine structure in the droplet spectrum. As with the O-H technique for sampling ice particles it is straightforward, and, for at least 5 years of cloud droplet sampling at the Elk Mountain Observatory, has provided the most consistent data set for droplet populations.



Fig. B1 Microphotograph of droplet craters on soot-coated glass slide used in the cloud gun.